


University of
Stavanger

FACULTY OF SCIENCE AND TECHNOLOGY

MASTER'S THESIS

Study programme/specialisation: Petroleum Engineering/Reservoir Engineering	Spring / Autumn semester, 2020. Open / Confidential
Author: Abdullah Numan Tahmiscioglu	
Programme coordinator: Supervisor(s): Skule Strand Tina Puntervold Iván Darió Piñerez Torrijos	
Title of master's thesis: Optimized Smart Water Composition at Ekofisk Conditions-Oil Recovery at High Temperatures	
Credits: 30	
Keywords: Smart Water Wettability Alteration Ekofisk Chalk Carbonates	Number of pages: + supplemental material/other : Stavanger, 15.12.2020..... date/year

Master's Thesis

Optimized Smart Water Composition at Ekofisk Conditions

Oil Recovery at High Temperature

By

Abdullah Numan Tahmisciođlu



Universitetet
i Stavanger

FACULTY OF SCIENCE AND ENGINEERING
DEPARTMENT OF ENERGY RESOURCES

December 15, 2020

Abstract

Seawater has been performing as a wettability modifier in chalk reservoirs and has been used for a long time. This wettability alteration enhances microscopic then overall displacement efficiencies. Having wettability altering capability makes seawater possible to spontaneously imbibe into the chalk matrix and produce extra oil. Studies show that Ca^{+2} , SO_4^{-2} , and Mg^{+2} , potential determining ions, can be chemically active and desorbs the organic oil acids from the chalk mineral surface. This release provides a more water-wet wetting condition to the reservoir.

Smart Water is a designed injection brine that can modify reservoir wettability towards water wet. Knowing that seawater already functioning as a Smart Water in chalk reservoirs, to design ideal Smart water, seawater is considered as a base injection brine. Smart Water for chalk needs to be abundant in Ca^{+2} , SO_4^{-2} , and Mg^{+2} concentrations. It is also shown that low Na^+ and Cl^- concentrations lead to better displacement performance. The wettability alteration capability of a Smart Water is directly related to reservoir temperature. Although slight Smart Water effect may be observed in low temperatures ~ 90 °C, as temperature increases to ~ 130 °C significant wettability alteration by Smart Water is observed.

In this thesis, finding a Smart Water composition and concentration, and stable equilibrium condition of the Smart Water is aimed. Stevns Klint Chalk cores used for its analogy importance to Ekofisk. Experiment temperature is also chosen as reservoir temperature of Ekofisk, 130 °C to provide a better resemblance.

Totally four cores cleaned with de-ionized water, restored 10% S_{wi} with sulfate-free formation water, and 90% S_{oi} with an oil with AN:0.53 mgKOH/g. All cores aged for 14 days at 130 °C. After a batch test was done Smart Water is decided to be prepared as a 10 M CaSO_4 solution. All cores spontaneously imbibed, by FW in secondary mode by SW and CaSO_4 solution-Smart Water in secondary and tertiary mode.

Spontaneous imbibition test with FW recovered 30% while SW 58% and CaSO_4 30% of OOIP in secondary mode. In tertiary mode, CaSO_4 showed a slight wettability alteration and recovered an extra 8% while SW performed very well wettability modification and recovered 55% of OOIP after 30% of FW.

SW also experimented in tertiary mode after CaSO_4 solution-Smart Water and recovered 54% of OOIP confirming its wettability alteration capabilities.

Acknowledgments

I would like to express my great appreciation to Professor Skule Strand and Professor Tina Puntervold for providing me this research opportunity and the invaluable guidance that they offered all the time.

I would like to address my sincere gratefulness to Dr. Iván Darió Piñerez Torrijos for offering constant support, deep knowledge, and being a selfless teacher.

I also offer my profound gratitude to Tolgahan Aydiner and Bekir Aydemir and my family for supporting my being without a rest.

I lastly would like to honor Alexandra Elbakyan for being a great motivation to me with her unshakeable stance

List of Figures

FIGURE 3.1 THE SIMPLIFIED POROUS MEDIUM AS A PACK OF PARALLEL CAPILLARY TUBES (LINDANGER, 2019)	27
FIGURE 3.2-DISPLACEMENT OF OIL BY WATERFLOODING FOR (A) OIL-WET, AND (B) WATER-WET MINERAL SURFACES. (STRAND, 2005)	30
FIGURE 3.3 CONTACT ANGLE MEASUREMENT (LINDANGER, 2019)	32
FIGURE 3.4 CAPILLARY PRESSURE CURVES FOR AMOTT AND AMOTT-HARVEY METHODS	34
FIGURE 3.5 ILLUSTRATION OF SPONTANEOUS IMBIBITION OF WATER	36
<i>FIGURE 3.6 TYPICAL CHROMATOGRAPHY WETTABILITY RESULT FOR A WATER-WET CARBONATE CORE</i>	38
<i>FIGURE 3.7 ILLUSTRATION OF SCN^- AND SO_4^{2-} IONS AROUND WATER-WET CARBONATE MINERAL SURFACE.</i>	38
<i>FIGURE 3.8 TYPICAL CHROMATOGRAPHY WETTABILITY RESULT FOR AN OIL-WET CARBONATE CORE</i>	38
<i>FIGURE 3.9 ILLUSTRATION OF SCN^- AND SO_4^{2-} IONS AROUND THE OIL-WET CARBONATE MINERAL SURFACE.</i>	38
FIGURE 4.1 OIL RECOVERY AT 120 °C BY SUCCESSIVE SPONTANEOUS IMBIBITION AND FORCED DISPLACEMENT (STRAND ET AL., 2008)	41
FIGURE 4.2 SI TESTS ON EQUALLY RESTORED CHALK CORES AT 90 °C. MODIFIED SW AS SMART WATER IMBIBING BRINES. (ZHANG, 2006)	42
FIGURE 4.3 SI TEST RESULTS ON EQUALLY RESTORED CHALK CORES AT 100 C	43
FIGURE 4.4 SI ON EQUALLY RESTORED CHALK CORES AT 70 C. SW BRINES WITH INCREASING CA CONCENTRATION AS IMBIBING BRINE.	43
FIGURE 4.5 SI TESTS DONE AT 70, 100 AND 130 °C. MODIFIED SW WITHOUT Ca^{+2} AND/OR Mg^{+2} WAS USED AS INITIAL IMBIBING BRINE AND LATER ON Mg^{+2} AND Ca^{+2} ADDED WITH A CONCENTRATION OF SW	44
FIGURE 4.6 OIL RECOVERY AT 90 °C BY SUCCESSIVE SPONTANEOUS IMBIBITION AND FORCED DISPLACEMENT	45

FIGURE 4.7 OIL RECOVERY AT 120 °C BY SUCCESSIVE SPONTANEOUS IMBIBITION AND FORCED DISPLACEMENT	45
FIGURE 4.8 SUGGESTED WETTABILITY ALTERATION MECHANISM WITH SEAWATER	46
FIGURE 6.1 CORE CLEANING RESULTS FOR ALL IONS FOR CORE #1	54
FIGURE 6.2 ION CHROMATOGRAPHY RESULTS FOR CORE CLEANING FOR $[SO_4^{-2}]$	55
FIGURE 6.3 ION CHROMATOGRAPHY RESULTS FOR CORE CLEANING FOR $[CA^{+2}]$	55
FIGURE 6.4 ION CHROMATOGRAPHY RESULTS FOR CORE CLEANING FOR $[MG^{+2}]$	55
FIGURE 6.5 ION CHROMATOGRAPHY RESULTS FOR CORE CLEANING FOR $[K^+]$	55
FIGURE 6.6 ION CHROMATOGRAPHY RESULTS FOR CORE CLEANING FOR $[NA^+]$	55
FIGURE 6.7 ION CHROMATOGRAPHY RESULTS FOR CORE.....	55
FIGURE 6.8 FREE SO_4^{-2} CONCENTRATION IN $CACO_3-H_2SO_4$ SOLUTIONS.....	59
FIGURE 6.9 FREE CA^{+2} CONCENTRATION IN $CACO_3-H_2SO_4$ SOLUTIONS.	60
FIGURE 6.10 OIL RECOVERY WITH SPONTANEOUS IMBIBITION BY FW -CORE#1	61
FIGURE 6.11 OIL RECOVERY WITH SPONTANEOUS IMBIBITION BY FW -CORE#6	62
FIGURE 6.12 OIL RECOVERY WITH SPONTANEOUS IMBIBITION BY FW/SW -CORE#6	63
FIGURE 6.13 OIL RECOVERY WITH SPONTANEOUS IMBIBITION BY FW/ $CASO_4$ -CORE#1	63
FIGURE 6.14 OIL RECOVERY WITH SPONTANEOUS IMBIBITION BY SW- CORE#2	64
FIGURE 6.15 OIL RECOVERY WITH SPONTANEOUS IMBIBITION BY $CASO_4$	65
FIGURE 6.16 OIL RECOVERY WITH SPONTANEOUS IMBIBITION BY $CASO_4/SW$	65
FIGURE 6.17 SI TEST RESULTS PERFORMED IN A STRONGLY WATER WET SK CHALK CORE	66

List of Tables

TABLE 3.1-CLASSIFICATION OF EOR METHODS.....	21
TABLE 3.2 WETTABILITY STATES FOR THE RANGE OF CONTACT ANGLES	32
TABLE 3.3 AMOTT HARVEY INDEX FOR DIFFERENT WETTING STATES.....	35
TABLE 5.1 MEASURED OIL PROPERTIES	48
TABLE 5.2 MEASURED CORE PROPERTIES.....	49
TABLE 5.3 BRINE COMPOSITIONS AND PROPERTIES.....	50
TABLE 6.1 POROSITY MEASUREMENT RESULTS	56
TABLE 6.2 PERMEABILITY MEASUREMENT RESULTS.....	57
TABLE 6.3 POROSITY AND PERMEABILITY SUMMARIZED RESULTS	58
TABLE 6.4 ION CHROMATOGRAPHY ANALYSIS OF THE EQUILIBRATED $CACO_3-H_2SO_4$ SOLUTIONS	59
TABLE 6.5 OIL RECOVERY BY SPONTANEOUS IMBIBITION ON SECONDARY AND TERTIARY MODE AT 130 °C.....	67
TABLE 8.1 OIL RECOVERY BY SPONTANEOUS IMBIBITION ON SECONDARY AND TERTIARY MODE AT 130 °C.....	70

Contents

Abstract	2
Acknowledgments	6
Table of Contents	Error! Bookmark not defined.
List of Figures	9
List of Tables.....	10
Symbols and Abbreviations	14
1 Introduction	18

2	Objective	19
3	Theory	20
3.1	Carbonate Reservoirs.....	20
3.2	Oil Recovery in Carbonate Rocks	20
3.3	Enhanced Oil Recovery	21
3.4	Displacement Efficiencies and Forces.....	22
3.4.1	Microscopic and Macroscopic Displacement	22
3.4.2	Fluid Flow in Porous Media.....	23
3.4.3	Capillary Forces	26
3.4.4	Gravity Forces	26
3.4.5	Viscous Forces	27
3.4.6	Capillary Number	28
3.5	Wettability	28
3.5.1	Wettability in Porous Media	29
3.5.2	Effects of Wettability	30
3.5.3	Wettability in Carbonates.....	31
3.6	Wettability Measurement	31
3.6.1	Contact Angle Measurement.....	31
3.6.2	Amott Harvey Method	33
3.6.1	Spontaneous Imbibition.....	36
3.6.2	Chromatographic Wettability Test	37
4	Water-Based EOR in Carbonates	40
4.1	Waterflooding.....	40
4.2	Wettability Alteration in Carbonate by Modifying the Ionic Composition of Water	40
4.2.1	Na ⁺ Effect.....	42
4.2.2	SO ₄ ²⁻ Effect.....	42
4.2.3	Ca ²⁺ Effect.....	43

4.2.4	Mg ⁺² Effect.....	44
4.2.5	Temperature Effect.....	45
4.3	Smart Water.....	46
5	Experimental Work.....	48
5.1	Materials.....	48
5.1.1	Oil.....	48
5.1.2	Core Material.....	48
5.1.3	Brines.....	49
5.2	Methodology.....	50
5.2.1	Core Cleaning.....	50
5.2.2	Porosity Measurement.....	50
5.2.3	Permeability Measurement.....	51
5.2.4	Establishing Initial Water Saturation.....	52
5.2.5	Establishing Oil Saturation.....	52
5.2.6	Aging Phase.....	53
5.2.7	Spontaneous Imbibition Test.....	53
5.2.8	CaCO ₃ -H ₂ SO ₄ Batch Test.....	53
6	Results.....	54
6.1	Core Cleaning.....	54
6.2	Porosity and Permeability Measurement.....	56
6.2.1	Porosity Measurement.....	56
6.2.2	Permeability Measurement.....	56
6.3	CaCO ₃ -H ₂ SO ₄ Batch Test.....	58
6.4	The efficiency of a Sulfuric Acid Based Smart Water.....	60
6.5	Spontaneous Imbibition.....	61
6.5.1	Initial core wettability.....	61
6.5.2	Tertiary Smart Water EOR Effects.....	62

6.5.3	Secondary Smart Water EOR Effects	64
6.5.4	Wettability Measurement	66
7	Discussions.....	68
8	Conclusion.....	70
	Appendixes.....	72
8.1	Spontaneous Imbibition Data	72
8.2	Core Cleaning Data	76
	Bibliography.....	79

Symbols and Abbreviations

A_{sample}	The area between SO_4^{-2} and SCN^- curves of the sample
A_{heptane}	The area between SO_4^{-2} and SCN^- curves completely water-wet reference core containing heptane
$E,$	Total displacement efficiency, fraction
$E_D,$	Microscopic displacement efficiency, fraction
$E_v,$	Macroscopic displacement efficiency, fraction
g	Gravitational acceleration, 9.8 m/s^2
H	Height of the fluid column, m

I_o	Amott index for oil, fraction
I_w	Amott index for water, fraction
I_w^*	Modified Amott water index, fraction
$k,$	Permeability, m^2
$k_{rw},$	Relative permeability of water, fraction
$k_{ro},$	Relative permeability of oil, fraction
L	Length of the capillary tube, m
$M,$	Mobility ratio, fraction
$J^*,$	Leverett dimensionless entry pressure
$PV,$	Pore volume, ml
$P_c,$	Capillary pressure, Pa
$P_{NW},$	The pressure of the non-wetting phase, Pa
$P_w,$	The pressure of the wetting phase, Pa
$r,$	Pore radius, m
$S_{or},$	Residual oil saturation, fraction
$S_{wi},$	Irreducible water saturation, fraction
$S_{oi},$	Initial oil saturation, fraction
$S_{wc} ,$	Connate water saturation, fraction
SI_C	OOIP% after spontaneous imbibition of water in the core to be evaluated, %
SI_{WWC}	OOIP% after spontaneous imbibition of water in the strongly water-wet core, %
$u,$	Darcy Velocity, m/s
WI	Wettability index

w_{target} ,	weight of the core with $S_w=10\%$, g
w_{dry} ,	weight of the dry core, g
ΔP_g	Pressure difference over the oil-water interface due to gravity, Pa
$\Delta \rho$	Difference in the density of the two phases, kg/m^3
ΔP	The pressure difference across the capillary tube, Pa
ΔS_{ws}	Water saturation change due to spontaneous imbibition of water, fraction
ΔS_{wf}	Water saturation change due to forced injection of water, fraction
ΔS_{os}	Water saturation change due to spontaneous imbibition of oil, fraction
ΔS_{of}	Water saturation change due to forced injection of oil, fraction
μ ,	Fluid Viscosity, Pa.s
μ_w ,	Water viscosity, Pa.s
μ_o ,	Oil viscosity, Pa.s
λ_w ,	Mobility of water, $\text{m}^2/\text{Pa.s}$
λ_o ,	Mobility of oil, $\text{m}^2/\text{Pa.s}$
λ_D ,	Mobility of the displacing fluid, $\text{m}^2/\text{Pa.s}$
λ_d ,	Mobility of the displaced fluid, $\text{m}^2/\text{Pa.s}$
$\frac{dP}{dx}$	Pressure gradient, Pa/m,
σ	Interfacial tension, N/m
φ	Porosity, fraction
σ	Interfacial tension between wetting and non-wetting phase, N/m
θ ,	Contact angle, degree
v_{ave}	Average flow velocity in the capillary tube, m/s

r	Radius of the capillary tube, m
v_o	Velocity, m/s
σ_{ow}	Surface tension between oil and water, mN/m
σ_{os}	Oil-solid interfacial tension, mN/m
σ_{ws}	Water-solid interfacial tension, mN/m
ρ_{VB0S}	Density of the VB0S Brine, 1.0224 g/cm ³

1 Introduction

In a world that energy demand increases historically, petroleum still holds its economically important yet environmentally controversial place on the energy supply behalf.

Petroleum extraction has never been uncostly. Furthermore, advanced improvements in technology that is used and extreme conditions that new fields are being sought, keep supporting the high cost of new explorations. Consequently producing proven reserves more efficiently, is getting more attention than ever. Increasing oil recovery in proven reserves is the essential way to accomplishes that.

Half of the world's oil stays in carbonate reservoirs. Due to their special nature, carbonate reservoirs tend to have high residual oil saturation in a fractured porous system that can not be produced easily with primal yet conventional recovery techniques. Just because of this, as a chemical enhanced oil recovery technique, Smart Water, has been kept researched carefully, observed, and experimented neatly.

In this master thesis research study, Smart Water has been investigated experimentally working to answer some questions asked and confirm or refute some of the answers given in the past.

2 Objective

This thesis study primarily aims to research an injection brine, Smart Water, that shows a wettability alteration effect for chalk carbonates at 130 °C and compare its oil recovery performance to the oil recovery performance of seawater for the same conditions.

The study also targets to find the ion composition and concentrations for the Smart Water that does not cause any precipitation in the pore water-rock-brine system and does function as a wettability modifier as a Smart Water is supposed to be.

Moreover, the study interests in the oil recovery performance of the Smart Water and seawater in both secondary and tertiary mode after formation water.

Finally, the thesis aims to compare the oil recovery performance of Smart Water in the secondary mode after seawater and oil recovery performance of seawater in the secondary mode after Smart Water and analyze any possible wettability alteration.

3 Theory

3.1 Carbonate Reservoirs

Carbonate rocks are sedimentary rocks that are made mostly of carbonate minerals. These carbonate minerals are originated from calcareous organisms and animal debris. Due to the diversity of composition, it is useful to classify carbonate minerals so that elemental compositions show. Calcite (CaCO_3), Siderite (FeCO_3), Magnesite (MgCO_3), Dolomite (CaMgCO_3) and Ankerite ($\text{CaFe}(\text{CO}_3)_2$) are the carbonate minerals that make different carbonate rocks (Punternold, 2008). For instance, limestone is classified as carbonate rock with %50 or more Calcite mineral while carbonate rock with %50 or more dolomite mineral is classified as dolomite.

Carbonate rocks, together with other necessary elements and processes, may constitute carbonate reservoirs and may host hydrocarbons. The carbonate reservoirs hold approximately 50% of petroleum reserves (Treiber & Owens, 1972).

3.2 Oil Recovery in Carbonate Rocks

Oil production is conventionally being done under three stages, primary recovery, secondary recovery, and tertiary recovery. Primary recovery is the stage that the reservoir is produced with the energy stored in it. This energy may be one or combinations of solution gas drive, gas cap drive, gravity drive, rock expansion, aquifer expansion, or fluid expansion (Green & Willhite, 1998).

Secondary recovery starts when the primary recovery driving mechanisms begin to lose their energy and need to be pressure supported. This support is typically in the practice of water or gas injection. Different fluids are being injected from injection wells to displace oil towards the production wells (Green & Willhite, 1998). In the secondary recovery stage, the average hydrocarbon recoveries range between 20-40% of the original oil in place (Muggeridge et al., 2014).

Tertiary recovery term is used to cover all recovery enhancement techniques that can be designed and performed in addition to secondary recovery methods. Although primary,

secondary, and tertiary terms imply a sequential order due to their conventional applications, these stages are not necessarily in order. For instance, a secondary recovery method of water flooding can be performed starting from the first day of production. To clarify the misconception among the terms, enhanced oil recovery, EOR term is being more used and accepted by the community (Green & Willhite, 1998) and can be studied under categories of chemical methods, gas EOR methods, thermal methods, chemical methods, and emerging new methods

3.3 Enhanced Oil Recovery

EOR focuses on extracting more oil from already existing oil fields that experience production declines. Being working on already existing fields gives EOR the chance to save a substantial amount of capital from exploration expenditures. In a world that oil has a 31.6% share of the total global energy supply as a source (IEA, 2018), EOR still holds its important place in an industry that is in decline in discovering new giant oil fields (Cook, 2013).

Over decades, although people from diverse backgrounds, suggested EOR solutions from a different point of view, EOR methods happen to aim at least one of mobility ratio reduction, interfacial tension reduction, and wettability alteration principles to increase oil recovery. Table 3.1 classifies these EOR methods under four categories (Torrijos et al., 2017).

Table 3.1-Classification of EOR Methods

Chemical Methods	Surfactant Flooding Polymer Flooding Alkaline Flooding Alkaline-Surfactant-Polymer (ASP) Flooding Gels for Water Diversion/Shut-off Solvent Flooding
Gas EOR Methods	Hydrocarbon Injection (Miscible/Immiscible) CO ₂ Flooding (Miscible/Immiscible) Nitrogen Flooding Flue Gas Injection (Miscible/Immiscible) Water Alternating Gas (WAG)

Thermal Methods	Steam Flooding Cycle Steam Stimulation In-situ Combustion Hot Water Flooding Steam Assisted Gravity Drainage
Emerging EOR Methods	Smart Water Low Salinity Waterflooding Carbonated Waterflooding Microbial EOR Enzymatic EOR Electromagnetic Heating Surface Mining and Extraction Nano Particles

3.4 Displacement Efficiencies and Forces

3.4.1 Microscopic and Macroscopic Displacement

The total displacement efficiency is defined as the product of microscopic and macroscopic displacement efficiencies. The total displacement efficiency is defined as follows,

$$E = E_D E_v \tag{3.1}$$

Where

E , Total displacement efficiency, fraction

E_D , Microscopic displacement efficiency, fraction

E_v , Macroscopic displacement efficiency, fraction

Equation 3.1 summarizes that the closer E gets to the 1, the higher the displacement efficiency of oil the displacement will have. In Equation 3.1, E_D represents mobilization of oil in pore scale and directly related to S_{or} while E_v represents how well displacement progresses through the reservoir, volumetrically.

EOR processes are often about decreasing the S_{or} then increasing E_D . While S_{or} is dictated by chemical and physical relations between oil, water, and rock; IFT and wettability alteration emerge as important concepts to decrease the S_{or} then increase E_D . Equation 3.2 shows how E_D and S_{or} relates.

$$E_D = \frac{S_{oi} - S_{or}}{S_{oi}} \quad 3.2$$

Where

E_D , Microscopic displacement efficiency, fraction

S_{oi} , Initial oil saturation, fraction

S_{or} , Residual oil saturation, fraction

On the other hand, E_v is resulted from macro factors like reservoir geometry and structure, viscosity ratio, and density differences of displacing and displaced fluids. An unfavorable reservoir geometry, high density, and viscosity differences cause high mobility ratios and poor flooding performance hence early water breakthrough. But ideally, E_D is being studied to be increased by creating a uniform flood front with a low mobility ratio to have a late water breakthrough.

3.4.2 Fluid Flow in Porous Media

Darcy's fluid flow law constructs the relation between porous medium and fluid that flows through it. Darcy's law, Equation 3.3 defines the permeability of the porous medium by measuring the flow rate and the pressure difference between flow inlet and outlet.

$$u = -\frac{k}{\mu} \frac{dP}{dx} \quad 3.3$$

Where

u , Darcy Velocity, m/s

k , Permeability, m²

μ , Fluid Viscosity, Pa.s

$\frac{dP}{dx}$, Pressure gradient, Pa/m,

In a waterflooding case, water is displacing and oil is being displaced, viscosities of the fluids and the wettability determine the mobility of the phases in the presence of the other phase (Torrijos et al., 2017). Mobility of water and oil phases are defined as follows in Equation 3.4 and 3.5

$$\lambda_w = \left(\frac{k_{rw}}{\mu_w} \right) S_{or} \quad 3.4$$

$$\lambda_o = \left(\frac{k_{ro}}{\mu_o} \right) S_{wi} \quad 3.5$$

Where

λ_w , Mobility of water, m²/ Pa.s

λ_o , Mobility of oil, m²/ Pa.s

k_{rw} , Relative permeability of water, fraction

μ_w , Water viscosity, Pa.s

k_{ro} , Relative permeability of oil, fraction

μ_o , Oil viscosity, Pa.s

S_{or} , Residual oil saturation, fraction

S_{wi} , Irreducible water saturation, fraction

In addition to mobilities, the ratio of phase mobilities become practical to qualify how phases move together in the presence of the other.

The mobility ratio, M is defined as follows.

$$M = \frac{\lambda_D}{\lambda_d} = \frac{\lambda_w}{\lambda_o} = \frac{\left(\frac{k_{rw}}{\mu_w}\right)_{S_{or}}}{\left(\frac{k_{ro}}{\mu_o}\right)_{S_{wi}}} \quad 3.6$$

Where

M , Mobility ratio, fraction

λ_D , Mobility of the displacing fluid, $m^2/ Pa.s$

λ_d , Mobility of the displaced fluid, $m^2/ Pa.s$

λ_w , Mobility of water, $m^2/ Pa.s$

λ_o , Mobility of oil, $m^2/ Pa.s$

k_{rw} , Relative permeability of water, fraction

μ_w , Water viscosity, Pa.s

k_{ro} , Relative permeability of oil, fraction

μ_o , Oil viscosity, Pa.s

S_{or} , Residual oil saturation, fraction

S_{wi} , Irreducible water saturation, fraction

In fractured carbonate reservoirs, spontaneous imbibition rules the recovery mechanism, and the wettability of the mineral surface determines most of its efficiency. In an oil-wet system, due to having capillary pressure working against the oil displacement, imbibing fluid needs to overcome a capillary entry pressure to the matrix. The Leverett J-function claims to calculate this capillary entry pressure as follows

$$P_c = \sigma \sqrt{\frac{\phi}{k}} J^* \quad 3.7$$

Where

- P_c , Capillary pressure, Pa
- σ , Interfacial tension, N/m
- φ , Porosity, fraction
- J^* , Leverett dimensionless entry pressure ($J^* \approx 0.25$ for completely water wet and)

3.4.3 Capillary Forces

Capillary pressure is the pressure difference between two sides of the interphase of two immiscible fluids. (Green & Willhite, 1998). Capillary force is the force that determines the fluid distribution and displacement in a reservoir system. Capillary forces also are affected by geometry and dimensions of pore throats, wettability, and interfacial tension. Capillary forces can work in favor of oil displacement in a fractured reservoir while in a non-fractured reservoir it can cause oil trapping and increase residual oil saturation, it is defined as follows.

$$P_c = P_{NW} - P_W = \frac{2\sigma\cos\theta}{r} \quad 3.8$$

Where

- P_c , Capillary pressure, Pa
- P_{NW} , The pressure of the non-wetting phase, Pa
- P_W , The pressure of the wetting phase, Pa
- σ , Interfacial tension between wetting and non-wetting phase, N/m
- θ , Contact angle, degree
- r , Pore radius, m

3.4.4 Gravity Forces

Gravity forces are the gravitational forces that are exerted on fluids. In the case of having large density differences between fluids, and low oil-water interfacial tension conditions they become significant. Gravity force difference can be calculated as follows

$$\Delta P_g = \Delta\rho gH \quad 3.9$$

Where

ΔP_g Pressure difference over the oil-water interface due to gravity, Pa

$\Delta\rho$ Difference in the density of the two phases, kg/m³

g Gravitational acceleration, 9.8 m/s²

H Height of the fluid column, m

3.4.5 Viscous Forces

During fluid flow in porous media, flow faces a resistance. The resistance depends on the properties of the porous medium and the flow itself. The viscous forces are reflected as a pressure drop (Green & Willhite, 1998). For the sake of simplification, the porous medium is regarded as a pack of many parallel capillary tubes that laminar flow happens to be in them. Pressure drop due to viscous forces is calculated as in Equation 3.10.

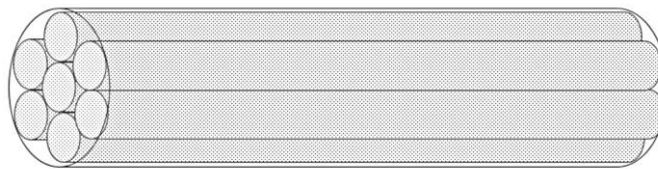


Figure 3.1 The simplified porous medium as a pack of parallel capillary tubes (Lindanger, 2019)

$$\Delta P = -\frac{8\mu L v_{ave}}{r^2 g_c} \quad 3.10$$

Where

ΔP The pressure difference across the capillary tube, Pa

μ Viscosity, Pa.s

L Length of the capillary tube, m

v_{ave} Average flow velocity in the capillary tube, m/s

r Radius of the capillary tube, m

3.4.6 Capillary Number

Capillary number, N_c is the dimensionless ratio of viscous forces to capillary forces. If viscous forces dominate the porous flow, the capillary number increases leading residual oil saturation to decrease. And it becomes smaller if the flow is capillary force dominated. As the capillary number gets smaller, it can indicate that oil might get capillary trapped and increase the residual oil saturation. The capillary number is calculated as in Equation 3.11 (Moore & Slobod, 1955)

$$N_c = \frac{\mu_w v_o}{\sigma_{ow} \cos\theta} \quad 3.11$$

Where

μ_w Water viscosity, mPa.s

v_o Velocity, m/s

σ_{ow} Surface tension between oil and water, mN/m

θ Contact angle, degree

3.5 Wettability

Wettability is described by being the tendency of a fluid to spread on a solid rock surface in the presence of other immiscible fluids and it is known to be one of the major factors affecting multiphase flow properties, fluid distribution in porous media (Craig, 1971; Koval, 1992). Aging, temperature, and the surface charge affect the wettability behavior of a mineral surface to a certain fluid. (Strand, 2005). Wettability is also known for changing oil displacement efficiencies by affecting relative permeability curves, capillary pressure, and finally residual oil saturation (Anderson, 2013). Hence altering the wettability in a way that oil displacement efficiencies improve, is a great interest for those who aim to improve oil recovery.

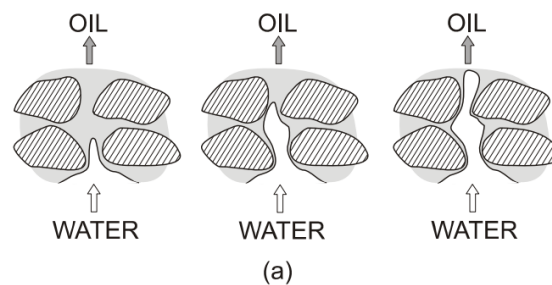
3.5.1 Wettability in Porous Media

For the scope of petroleum studies, in the co-existence of two immiscible fluids, oil, and water, wettability is conceptualized between two extremes of being strongly oil-wet and being strongly water-wet. All porous sedimentary medium is known to be originally water-wet due to lack of oil presence. After oil migrates, factors that determine the wettability state change and reach an equilibrium at which the initial wettability state of the reservoir establishes.

The wettability behavior of the mineral surface is not necessarily homogenous for all across the reservoir. The rock happens to have a heterogeneous wettability if specific mineral surface regions have a specific affinity to water or oil. In this fractional wetting condition, rock is partially oil-wet and partially water-wet for the different parts of the rock surface.

In a strongly oil-wet porous system, the oil covers most of the rock surface creating a thin oil film on the mineral surface of the rock. Oil fills small pore spaces and forces water to be in the middle of the larger pores. During water flooding, as shown in Figure 3.2(a) water does not reach these small pores and flows mainly through the larger pores. This causes poor oil displacement efficiencies and high residual oil saturation.

Contrarily, in a strongly water-wet porous system, water covers most of the rock surface and fills small pores, leaving oil in the larger pores. During water flooding, oil volumes in the larger pores might get trapped in Figure 3.2(b). (Strand, 2005)



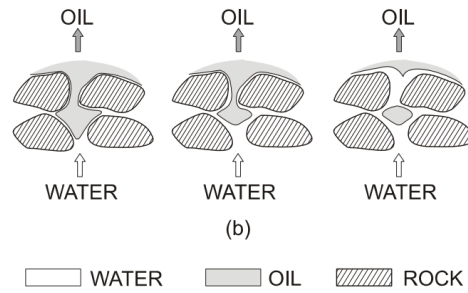


Figure 3.2-Displacement of oil by waterflooding for (a) oil-wet, and (b) water-wet mineral surfaces. (Strand, 2005)

Among many factors determining the wettability profile of a porous system, crude oil components and mineral composition can be named as two of the most important factors. Asphaltene and resin groups in crude oil are known to be affecting wetting due to polar molecules in them that show acidic or basic character by nature (Anderson, 1986; Buckley, 1996)

Mineral composition interaction with polar components differs from sandstone to carbonate rocks. (Buckley & Liu, 1998; Denekas et al., 1959). The carbonate mineral surface is generally positively charged below pH 8-9 and attracts negatively charged surface-active ions. If the mineral surface adsorbs negatively charged acidic oil components it becomes more oil-wet (Pierre et al., 1990). Sandstone mineral surface, on the other hand, charged negatively above pH 2 (Menezes et al., 1989) and adsorbs basic oil components and positively charged surface-active ions. (Cuiec, 1984; Kowalewski et al., 2003; Torsæter & Silseth, 1985). If basic oil components get adsorbed to sandstone mineral surface, it becomes more oil-wet.

3.5.2 Effects of Wettability

Understanding wettability in a porous system is important due to its critical effects on multiphase flow, fluid distribution, and phase trapping. Wetting is also found in direct relation to the capillary pressure, relative permeability, electrical properties, irreducible saturation, and many EOR processes (Strand, 2005).

3.5.3 Wettability in Carbonates

Most of the reservoir minerals are originally strongly water-wet due to the absence of polar components in the porous system. However, with oil intrusion along with the other factors, the wettability profile changes to set the initial wettability of the rock mineral to oil or water. Due to their mineral characteristics, carbonate rocks tend to be neutral to oil-wet (Chilingar & Yen, 1983; Treiber & Owens, 1972). Along with being oil-wet, carbonate reservoirs are also known to be challenging because of their fractured nature. In an oil-wet reservoir, high permeable fracture networks dominate fluid flow through the medium while tight matrix blocks are partially flow-wise isolated and keeping the oil within them with strong capillary forces. This results in the injection water not being able to imbibe sufficiently to the oil-bearing rock matrix. In these reservoirs, water injection does not function as efficiently as it does so in water-wet reservoir systems. (Strand, 2005).

Wettability is being determined depending on many factors and parameters (Standnes, 2001). Functional polar components in the crude oil, and the water solubility of polar oil components, surface charge and mineral composition of the rock (Anderson, 2013; Buckley et al., 2013), brine salinity and concentration of potential determining ions (Buckley, 1996), capillary pressure and thin-film forces, disjoining pressure (Hirasaki, 1991), the ability of the oil to stabilize heavy components (Al-Maamari & Buckley, 2013), temperature, pressure (Al-Maamari & Buckley, 2013), initial water saturation (Jadhunandan & Morrow, 2013) are major factors and parameters that determine the wettability state.

3.6 Wettability Measurement

Being such an important parameter for waterflooding design, makes wettability measurement crucial as well. There are many different approaches developed over the years to measure wettability. Three of them are presented as follows.

3.6.1 Contact Angle Measurement

The main approach to determine the wetting state and quantify it is doing so by contact angle measurement (Yuan & Lee, 2013). In a model wetting environment, rock is cut, the rock surface is smoothed then exposed to two immiscible fluids. After fluids settle on the rock surface, the contact angle is measured through the denser phase as in Figure 3.3.

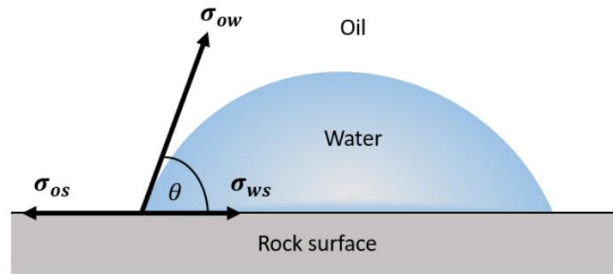


Figure 3.3 Contact angle measurement (Lindanger, 2019)

The static equilibrium in Figure 3.3 can be defined by Young's equation, Equation 3.12 which was developed on a thermodynamic basis stated by Gibbs (Letellier et al., 2007).

$$\sigma_{os} = \sigma_{ws} + \sigma_{ow} \cos \theta \quad 3.12$$

Where

σ_{os} Oil-solid interfacial tension, mN/m

σ_{ws} Water-solid interfacial tension, mN/m

σ_{ow} Oil-Water interfacial tension, mN/m

θ Contact angle measured through the denser phase, degree

Wettability states that can be interpreted by contact angle measurement ranges are presented in Table 3.2.

Table 3.2 Wettability states for the range of contact angles

Contact angle, degree	Wettability
0-30	Strongly water wet
30-90	Water wet
90	Neutral wet
90-150	Oil wet
150-180	Strongly oil-wet

Although contact angle theory is fundamental to understand wettability, contact angle measured on model surfaces is not representative to practice it for real reservoir rock oil-brine systems. Moreover, contact angle measurement is not easily applicable in reservoir rock pore space due to large fluid droplets that will not fit into nanometer or micrometer diameter pores. Also analyzing images taken to measure contact angle is not applicable even by using micro CT. These problems bring the need for other methods to measure wettability.

3.6.2 Amott Harvey Method

Amott proposed a quantitative method to calculate the average wettability of a core by measuring water saturation and capillary pressure through five imbibition and drainage processes (Amott, 1959).

As presented in Figure 3.4, the measurement starts with the primary drainage of oil which is oil injection (arrow 1) into a core that is entirely saturated with water. In the beginning, oil enters through the widest pores at the injection inlet after overcoming the capillary entry pressure and then oil finds a connected pathway through the system with an invasion percolation like flow. As oil occupies smaller pores it needs to pass through smaller pore throats hence face with larger capillary pressure. At the end of the injection core still has some water (S_{wc}) that can not be displaced by oil injection.

Measurement continues with spontaneous imbibition of water (arrow 2) where water fills the water wet regions of the pore space preferentially till capillary pressure becomes zero. Then forced water injection (arrow 3) occurs where water displaces the oil till water saturation becomes equal to $1-S_{or}$. Later, oil spontaneously imbibe (arrow 4) into the core, displaces the water till capillary pressure reaches zero. Lastly, secondary drainage (arrow 5) takes place and oil displaces water till water saturation becomes S_{wc} . Along with all the imbibition and drainage processes, water saturation values are recorded where capillary pressure becomes zero. Hence Amott index for water, I_w and oil, I_o are defined and calculated as in Equation 3.13 and Equation 3.14

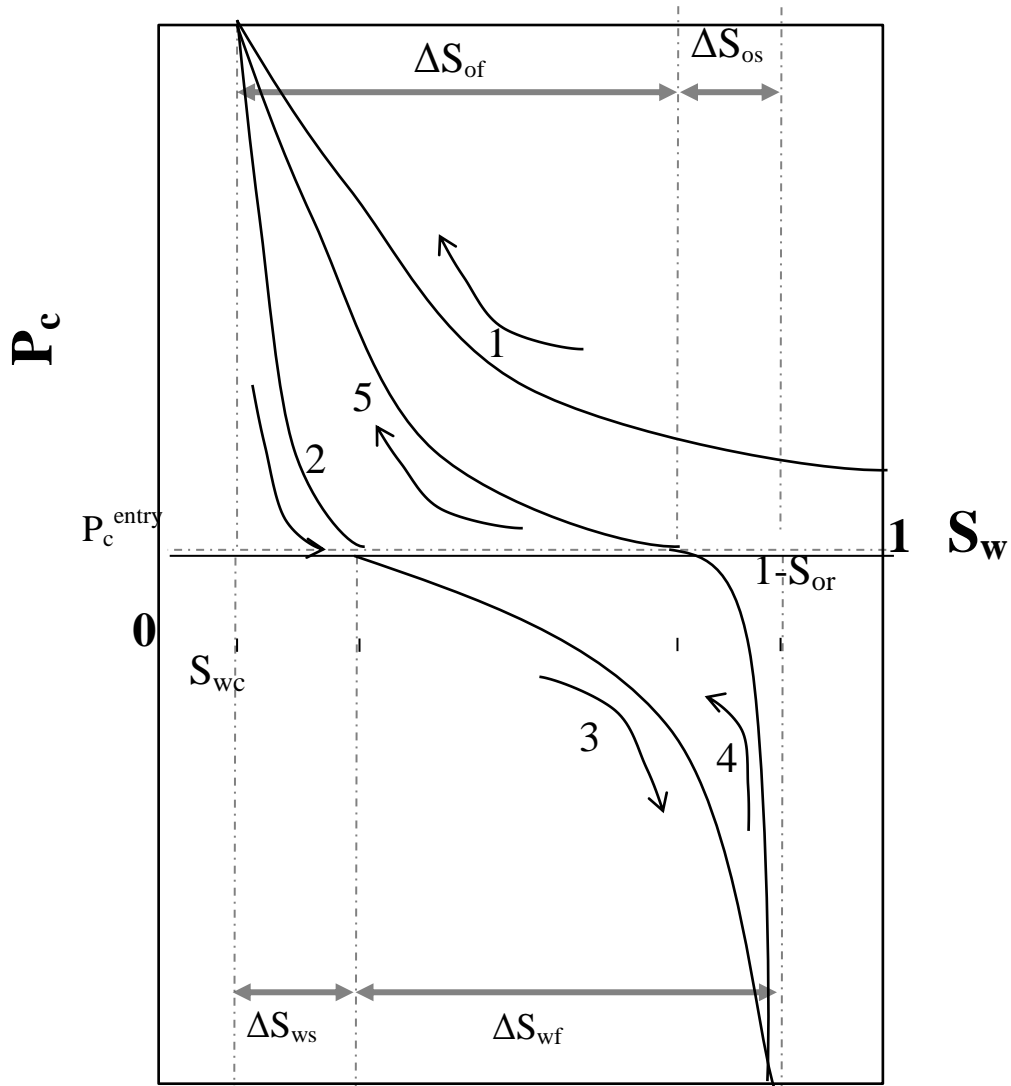


Figure 3.4 Capillary pressure curves for Amott and Amott-Harvey Methods

$$I_w = \frac{\Delta S_{ws}}{\Delta S_{ws} + \Delta S_{wf}} \quad 3.13$$

Where

I_w , Amott index for water, fraction

ΔS_{ws} , Water saturation change due to spontaneous imbibition of water, fraction

ΔS_{wf} , Water saturation change due to forced injection of water, fraction

$$I_o = \frac{\Delta S_{os}}{\Delta S_{os} + \Delta S_{of}} \quad 3.14$$

Where

I_o , Amott index for oil, fraction

ΔS_{os} , Water saturation change due to spontaneous imbibition of oil, fraction

ΔS_{of} , Water saturation change due to forced injection of oil, fraction

And

S_{wc} , Connate water saturation, fraction

S_{or} , Residual oil saturation, fraction

The Amott Harvey Index is defined as in Equation 3.15 using Amott indices as defined above

$$I_{AH} = I_o - I_w \quad 3.15$$

The Amott Harvey index ranges between -1 and 1 for the extremes of wettability states. Ranges for the Amott Harvey index are presented as follows (Cuiec, 1984).

Table 3.3 Amott Harvey index for different wetting states

I_{AH}	Wettability state
$-1 \leq I_{AH} \leq -0.3$	Oil-wet
$-0.3 < I_{AH} < 0.3$	Mixed-wet
$0.3 \leq I_{AH} \leq 1$	Water-wet

3.6.1 Spontaneous Imbibition

Spontaneous imbibition is a simplistic and qualitative way of measuring wettability in comparison to a reference wetting, preferentially a strongly water-wet or a strongly oil-wet core. The application starts with a core with initial water saturation. The core is immersed in imbibing water. The produced oil volume is recorded as a function of time. The production rate is compared to a reference strongly water-wet core. If spontaneous imbibition of water does not occur then similarly, the core at residual oil saturation is immersed in imbibing oil, and produced water volume is recorded as a function of time. The production rate is compared to a reference strongly oil-wet core.

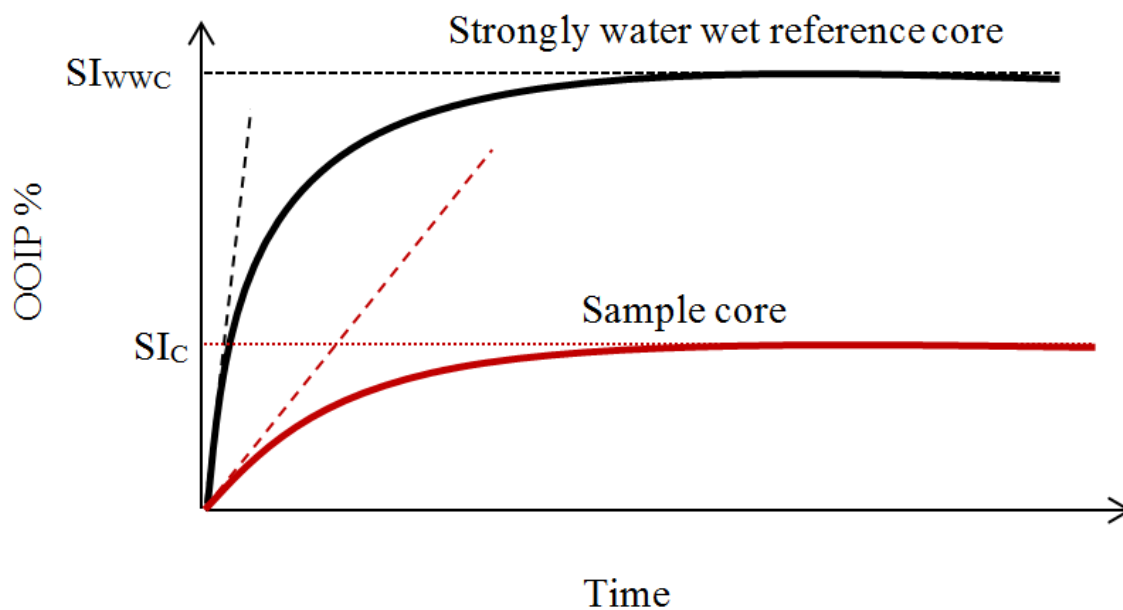


Figure 3.5 Illustration of spontaneous imbibition of water

The degree of wettability compare to the reference code can be calculated by using the modified Amott water index as follows (Zhou et al., 1996).

$$I_w^* = \frac{SI_c}{SI_{wwc}} \quad 3.16$$

Where

I_W^*	Modified Amott water index, fraction
SI_C	OOIP% after spontaneous imbibition of water in the core to be evaluated, %
SI_{WWC}	OOIP% after spontaneous imbibition of water in the strongly water-wet core, %

In the interpretation of the modified Amott index results, $I_W^*=1$ indicates evaluation core is strongly water wet, while $I_W^* = 0$ hints that the evaluation core is neutral wet.

3.6.2 Chromatographic Wettability Test

A recent method has been proposed to measure the wettability of carbonate cores (Skule Strand et al., 2006). Chromatographic wettability test unlike Amott's method and spontaneous imbibition method focuses on mineral surface chemistry. The method relies on water flooding a core with known concentrations of SO_4^{-2} and SCN^- . Flooding effluents are analyzed later to see SO_4^{-2} and SCN^- concentration. The method is designed upon SO_4^{-2} ions are getting adsorbed on water-wet carbonate mineral surfaces where SCN^- being a non-absorbing ion as a tracer.

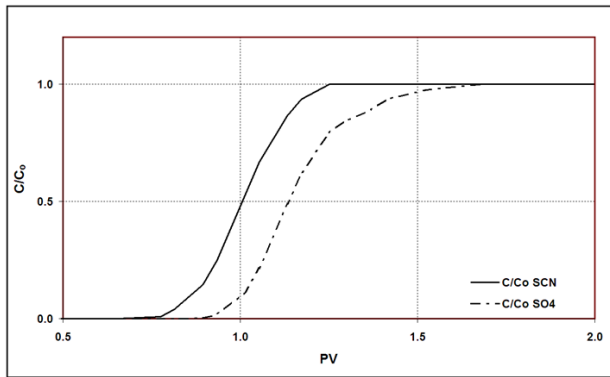


Figure 3.6 Typical chromatography wettability result for a water-wet carbonate core

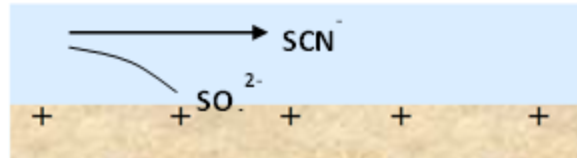


Figure 3.7 Illustration of SCN^- and SO_4^{2-} ions around water-wet carbonate mineral surface.

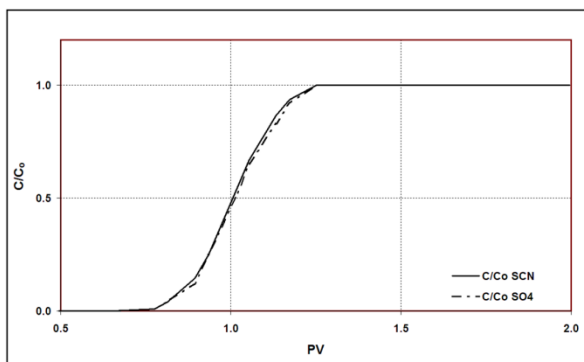


Figure 3.8 Typical chromatography wettability result for an oil-wet carbonate core

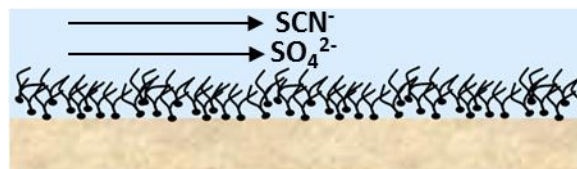


Figure 3.9 Illustration of SCN^- and SO_4^{2-} ions around the oil-wet carbonate mineral surface.

The wettability index is calculated as follows regarding the ratio of the area between SO_4^{2-} and SCN^- curves of the tested sample concentration difference in the flood profile, degree of water wetness is determined.

$$WI = \frac{A_{\text{sample}}}{A_{\text{heptane}}} \quad 3.17$$

Where

WI Wettability index

A_{sample} The area between SO_4^{2-} and SCN^- curves of the sample

A_{heptane} The area between SO_4^{2-} and SCN^- curves completely water-wet reference core containing heptane

In interpretation,

$WI_{new} = 1.0$ represents a completely water-wet system

$WI_{new} = 0.5$ represents an intermediate water-wet system

$WI_{new} = 0.0$ represents a completely oil-wet system.

4 Water-Based EOR in Carbonates

4.1 Waterflooding

Waterflooding has been widely accepted and practiced as a secondary recovery technique for a long time to provide pressure support to the reservoirs to slow down the production decline. Being studied and applied vastly made waterflooding possible to investigate its strong and weak sides. For example, it is shown that (Alvarez & Sawatzky, 2013) waterflooding is not efficient for heavy oil reservoirs as it is efficient for light and medium oil reservoirs. It is due to the low macroscopic displacement efficiency that occurs between the water and heavy oil phase. On the other hand, Wade studies (Wade, 1971) 53 waterflooding cases statistically and shows that waterflooding results in an average oil recovery of 23.3% off total pore volume while average primary oil recovery was 9.4%. This shows that oil recovery can be largely increased by applying waterflooding.

In addition to efficiencies, drawbacks that waterflooding designs might face also studied and seen that formation water-injection water compatibilities, scaling issues, corrosion control, sand production troubles are the some of the problems to be considered prior to the waterflooding planing.

Moreover, waterflooding was researched also with respect to injection water composition after seeing the results that not all water sources lead to similar oil displacement results. Hence, different injection waters have been studied to see their displacement efficiencies in flooding cases.

In carbonate reservoirs, seawater has been used in its availability as injection water and seen a vast improvement in oil displacement. Being a natural displacement enhancer in carbonate resevoirs, attracts lots of study attention to seawater and its composition.

4.2 Wettability Alteration in Carbonate by Modifying the Ionic Composition of Water

After being accepted and used as a good injection water for carbonates, seawater was researched regarding the mechanism that it affects oil displacement with. Knowing that seawater does not provide any significant macroscopic displacement efficiency enhancement on its own, researches focused on properties of seawater that affect microscopic efficiency, namely wettability of rock-brine-oil system.

Studies show that (S. Strand et al., 2006; Zhang & Austad, 2006; Zhang et al., 2007a) wetting state in the porous medium can be enhanced by flooding with water that ionic composition of which is selected or modified in the favor of flooding efficiencies. In fractured, chalk reservoirs, seawater was discovered to be a wettability altering flooding water that improves oil displacement (Strand et al., 2008). In Figure 4.1, Strand et al. experiment sequential spontaneous imbibition and viscous flooding with two equally restored chalk cores at 120 °C. The named C#6 was initially spontaneously imbibed with FW and resulted around 12% of OOIP. The core next changed its SI brine to SW and resulted in 18% of OOIP extra oil recovery. Having this recovery improvement shows that SW has a valid wettability modifier and acts as a Smart Water for chalk at 120 °C.

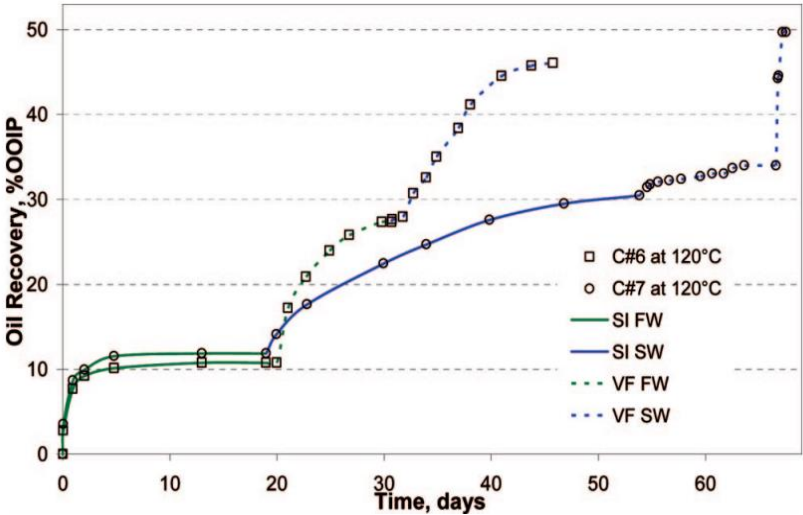


Figure 4.1 Oil recovery at 120 °C by successive spontaneous imbibition and forced displacement (Strand et al., 2008)

Zhang also studied (Zhang et al., 2007a) and showed by using equally restored chalk cores, how different injection brines affect oil displacement differently. In the study, as a base case FW with no sulfate was spontaneously imbibed into a core and around 18% of OOIP was recovered. To see SW effect on oil recovery. SW was used in spontaneous imbibition experiment and resulted in around 38 % of OOIP, giving extra 20 % of OOIP compare to FW. This shows how SW acts as a Smart Water in chalk cores at 90 °C and modifies wettability (Figure 4.2).

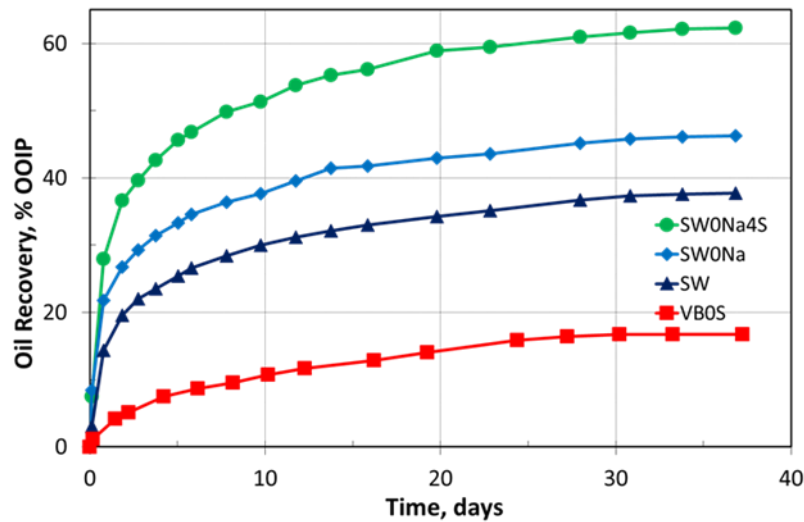


Figure 4.2 SI tests on equally restored chalk cores at 90 °C. Modified SW as Smart Water imbibing brines. (Zhang, 2006)

4.2.1 Na⁺ Effect

Zhang (Zhang, 2006) in the study also experiments how Na⁺ affects oil recovery by removing Na⁺ from injection brine of SW. A core was spontaneously imbibed at 90 °C with Na⁺ removed SW and around 10% of OOIP extra oil recovered compare to SW (Figure 4.2).. This indicates that removing Na⁺ from SW enhance wettability alteration capability of SW at 90 °C

4.2.2 SO₄⁻² Effect

In the same study (Zhang, 2006), SO₄⁻² effect is also tested. Zhang used a SW with no Na⁺ and spiked its SO₄⁻² concentration to four times of original as a imbibing brine. A core was spontaneously imbibed with this brine and seen that SW with no Na⁺ and four times spiked SO₄⁻² brine recovers extra 18% of OOIP compare to SW with no Na⁺, giving an ultimate recovery of 62% of OOIP (Figure 4.2). This confirms that SO₄⁻² is an important ion for wettability alteration and increasing its concentration, improves wettability alteration capability of SW at 90 °C.

Zhang also tested SO₄⁻² effect seprately as shown in the Figure 4.3 end confirms that SO₄⁻² concentration affects and enhance wettability modification capability of SW.

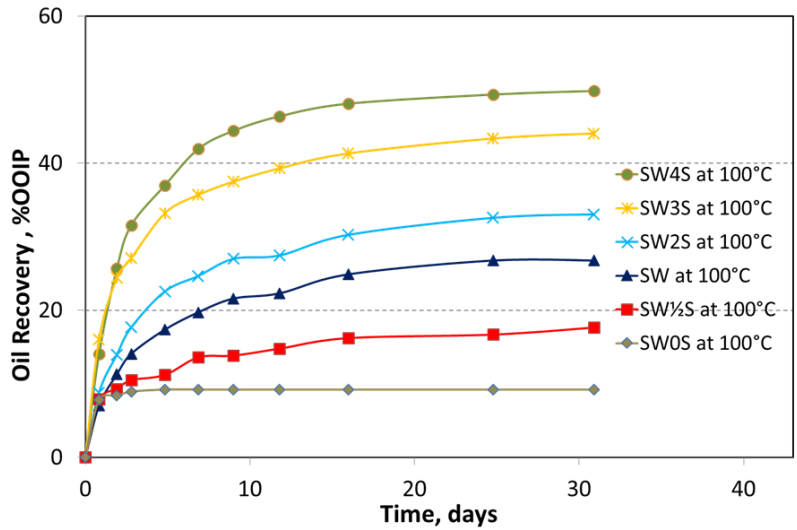


Figure 4.3 SI test results on equally restored chalk cores at 100 C

4.2.3 Ca⁺² Effect

Ca⁺² effect also has been researched by Zhang (Zhang, 2006). In the study, equally restored chalk cores have experimented with SI using five imbibing brines with different Ca⁺² concentrations at 70 °C. Imbibing brines were prepared based on SW. SI oil recovery results in Figure 4.4 show that increase in Ca⁺² concentration affect wettability alteration potential of SW significantly and results in better oil displacement and recovery.

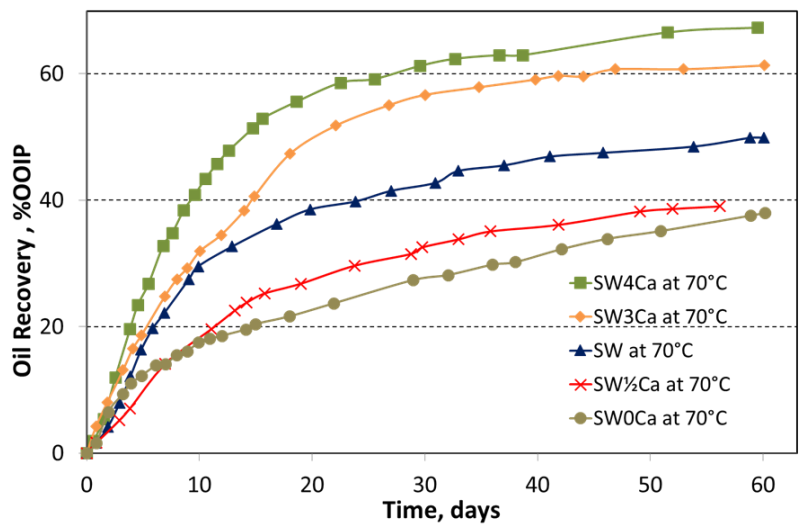


Figure 4.4 SI on equally restored chalk cores at 70 C. SW brines with increasing Ca concentration as imbibing brine.

4.2.4 Mg⁺² Effect

Zhang states (Zhang et al., 2007b) that another important ion for wettability alteration in carbonates is Mg⁺². In the study, equally restored chalk cores were SI tested with different brines and oil recovery results were presented in (Figure 4.5).

CM-1 core was spontaneously imbibed at 100 °C with a brine SW0 (no Ca⁺², no Mg⁺², 1x SO₄⁻²) resulted in around 12% of OOIP, and then on day 43, SW amount of Mg⁺² was added to the SI brine and resulted in extra 20% of OOIP compare to the SW0. This result shows that Mg⁺² has an wettability altering properties in chalk at 100 °C.

In the same study, Zhang also shows an interesting effect of Mg⁺². As shown in Figure 4.5, at 100 °C, SI shows similar results for CM-2 and CM-4 cores that were being imbibed with brines SW0-0S (no Ca⁺², no Mg⁺², no SO₄⁻²) and SW0-4S (no Ca⁺², no Mg⁺², 4xSO₄⁻²) respectively and giving around 12% OOIP. This shows in the absence of Ca⁺² and Mg⁺², SO₄⁻² loses its wettability modifying capability at 100 °C for chalk. Later in the same experiment, on day 53, SW amount of Mg⁺² was added to both of the imbibing brines to see Mg⁺² effect on both of the brines. Adding Mg⁺² to SW0-0S, resulted in extra 10% of OOIP while adding Mg⁺² to SW0-4S brine, resulted in extra 30% of OOIP. Even though adding Mg⁺² shows wettability alteration for both of the brines, a significant recovery difference was reported with the brine involving 4xSO₄⁻².

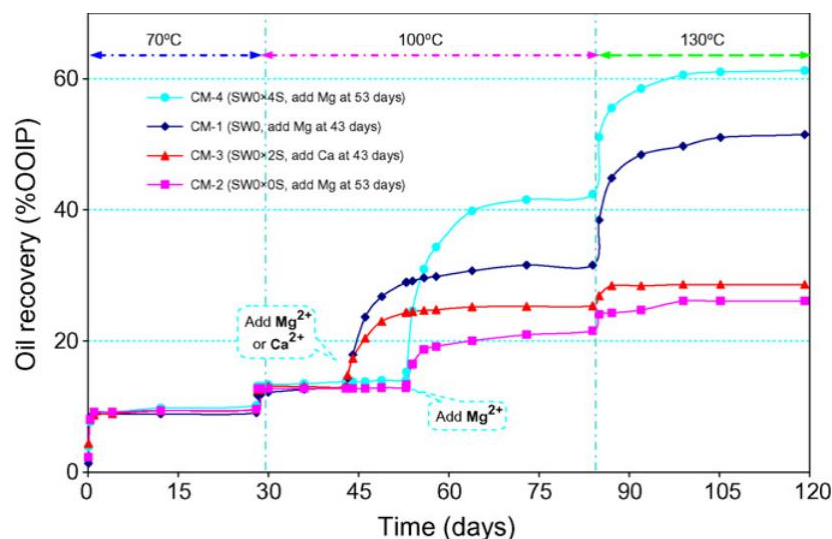


Figure 4.5 SI tests done at 70, 100 and 130 °C. Modified SW without Ca⁺² and/or Mg⁺² was used as initial imbibing brine and later on Mg⁺² and Ca⁺² added with a concentration of SW

4.2.5 Temperature Effect

Strand et al. (Strand et al., 2008) studied and showed the effect of temperature on wettability alteration with chalk core by using seawater sequentially with spontaneous imbibition and viscous flooding. As presented in Figure 4.6 and Figure 4.7, seawater at 90 °C with SI, has a very weak wettability modification capability showed by minor increase in oil recovery. The oil recovery was increased only by 2% of OOIP.

However, at 120 °C, seawater shows a powerful wettability modification for both spontaneous imbibition and viscous flooding as presented in Figure 4.7. At 120 °C, core C#6 is spontaneously imbibed with formation water recovering 12% of OOIP) and then imbibing brine was changed from FW to SW, giving a total recovery of 30% of OOIP. This extra 18% of OOIP oil recovery confirms that only by switching from formation water to seawater without any changes in the mobility ratio, Smart Water EOR effects are present.

Hence, wettability alteration on chalk cores by using seawater exists and is directly related to temperature. The wettability modification increases as temperature increases. (Strand et al., 2008)

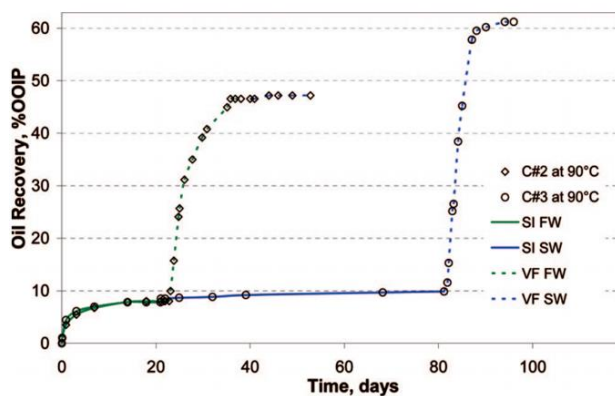


Figure 4.6 Oil recovery at 90 °C by successive spontaneous imbibition and forced displacement

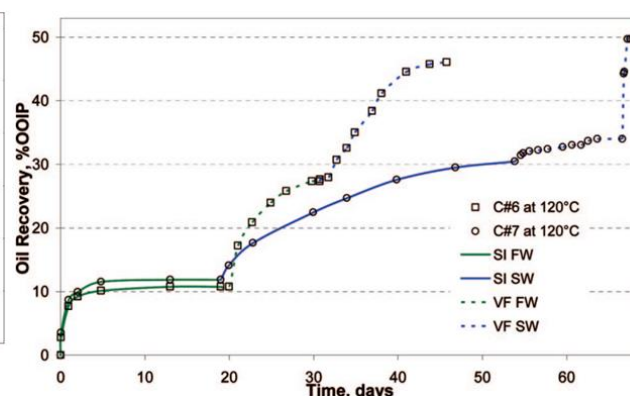


Figure 4.7 Oil recovery at 120 °C by successive spontaneous imbibition and forced displacement

4.3 Smart Water

An optimized Smart Water composition for chalk has previously been studied. Seawater behaves as a Smart Water at high temperatures. At lower temperatures, the efficiency of seawater could be improved based on the results (see Chapter 4.2)

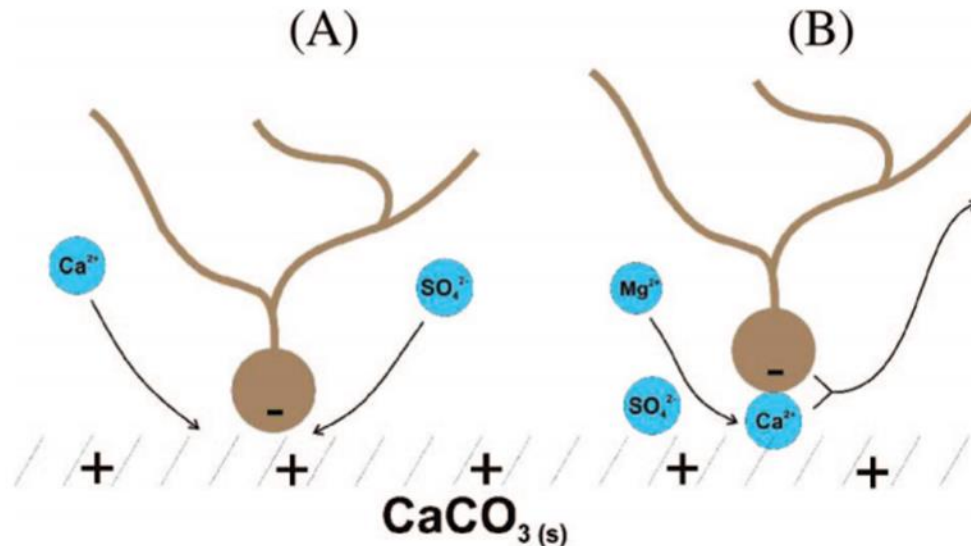


Figure 4.8 Suggested wettability alteration mechanism with seawater

Figure 4.8 illustrates the suggested (Torrijos et al., 2017) wettability alteration mechanism in chalk by seawater (A) when Ca^{+2} and SO_4^{-2} are active and (B) when Mg^{+2} and SO_4^{-2} are active at high temperatures.

Design of Smart Water for carbonates roughly relies on:

- Reduced concentration of NaCl
- An optimum concentration of SO_4^{-2} , Ca^{+2} and Mg^{+2}
- The optimum concentration should be considered as high enough to provide maximum wettability alteration and low enough not to cause any salt precipitation regarding temperature of interest.
- The Smart Water effect of Mg^{+2} should also not be overlooked and should be considered in the availability of Mg^{+2} such as Smart Water designs for dolomite reservoirs.

In the case of having access to pure water, low concentrated sulfuric acid can be prepared to produce an injection brine with a desired SO_4^{-2} and by injecting this brine to CaCO_3 reservoirs, desired Ca^{+2} concentration can be achieved due to CaCO_3 dissolution in the

near-wellbore of the injection well. As a result, it is suggested that a Smart Water with picked concentration of Ca^{+2} and SO_4^{-2} can be produced in-situ by H_2SO_4 injection to the chalk reservoirs.

In the next part, the efficiency of a sulfuric acid-based Smart Water is evaluated and compared with the efficiency of seawater at reservoir temperatures of 130 °C comparable to the Ekofisk field.

5 Experimental Work

5.1 Materials

5.1.1 Oil

A base oil, Res-40, was prepared by diluting Heidrun crude oil with n-heptane in a volume ratio of 60:40. Res-40 oil was treated with silica gel to remove surface-active components from it. After being treated with silica gel, Res-40 was centrifuged and filtered through a 0.5 μm Millipore filter. This treated oil was called Res-40-zero, implying it having very low surface-active components. Res-40 and Res-40-zero mixed regarding Equation 5.1 to obtain Oil-A with the acid number (AN)= 0.53 mgKOH/g and base number (BN)=0.31 mgKOH/g. Oil-A was used throughout the experiment.

$$AN_{Target} = AN_{Res-40} \times \frac{V_{Res-40}}{V_{Res-40} + V_{Res-40-zero}} + AN_{Res-40-zero} \times \frac{V_{Res-40-zero}}{V_{Res-40} + V_{Res-40-zero}} \quad 5.1$$

Table 5.1 Measured Oil Properties

Oil Name	Density (g/cm ³)	AN (mgKOH/g oil)	BN (mgKOH/g oil)	Viscosity (cP)
Res-40	0.82	1.85	0.67	2.7
Res-40-zero	0.81	0.01	0.03	2.4
Oil-A	0.81	0.53	0.31	2.5

5.1.2 Core Material

All cores that have been used in this research study, obtained from Stevns Klint outcrop chalk in Sjælland, Denmark. Cores were drilled in the same direction and from the same rock block. Cores were then shaven and cut into desired dimensions. The cores used in this research study are presented in Table 5.1. Core #1; Core #2; Core #4; Core#6 were used for oil recovery test while Core#5 was crushed into chalk powder to be used in CaCO₃-H₂SO₄ batch test.

Table 5.2 Measured Core Properties

Core Name	Length (cm)	Diameter (cm)	Bulk Volume (ml)	Pore Volume (ml)	Porosity (fraction)	k (mD)	Swi (%)	OOIP (ml)
Core #1	7.21	3.79	81.34	38.86	0.4778	4.08	10	34.97
Core #2	7.02	3.78	78.78	37.87	0.4807	4.00	10	34.08
Core #4	7.22	3.79	81.45	38.61	0.4741	3.61	10	34.75
Core #5	7.10	3.79	80.10	35.32	0.4410	3.77	-	-
Core #6	7.27	3.78	81.58	38.40	0.4707	3.93	10	34.56

5.1.3 Brines

Brines used in this research study prepared synthetically in the laboratory regarding the compositions in Table 5.3 Brine Compositions and Properties. To avoid possible precipitations during brine preparation, salts involving CO_3^{-2} , Cl^- , and SO_4^{-2} dissolved separately in de-ionized water. After visual assurance of having no salt precipitation in the mixtures, mixtures combined to obtain individual brines. Brines then were filtered through 0.22 μm Millipore filters.

5.1.3.1 Valhall brine

Valhall brine, the formation water characterized from the Valhall field located in the southern North Sea, was chosen in this research study to be studied with as formation water. Moreover, to see the possible effects of SO_4^{-2} on wettability and oil recovery, Valhall brine was prepared without any SO_4^{-2} in it and this brine was called Valhall brine zero sulfates (VB0S). VB0S was used as imbibing fluid for spontaneous imbibition tests for Core#1 and Core#6 besides being formation water as in initial water saturation for all cores studied.

5.1.3.2 Sea Water

Sea Water was prepared to be used as the imbibing fluid for the spontaneous imbibition test for Core#2 and Core#6.

5.1.3.3 CaSO_4 Solution-Smart Water

CaSO_4 solution was prepared regarding $\text{CaCO}_3\text{-H}_2\text{SO}_4$ batch test results to be used as the imbibing fluid for the spontaneous imbibition test for Core#4 and Core#1.

Table 5.3 Brine Compositions and Properties

Ions	FW (mM)	SW (mM)	Smart Water (mM)
HCO ₃ ⁻	9	2	0
Cl ⁻	1066	525	0
SO ₄ ⁻²	0	24	10
Mg ²⁺	8	45	0
Ca ²⁺	29	13	10
Na ⁺	997	450	0
K ⁺	5	10	0
Density, g/cm ³ at 20 °C	1.041	1.022	0.999
TDS, g/l	62.83	33.39	1.72
Ca ²⁺ /SO ₄ ²⁻	N/A	0.540	1

5.2 Methodology

5.2.1 Core Cleaning

Cores were cleaned with a procedure characterized by Puntervold (Puntervold et al.2007). Cores were flooded with 5 PV of de-ionized water with a flow rate of 0.1 ml/min at room temperature. Effluent samples were collected to test for both qualitatively to see SO₄⁻² presence in the effluent samples if there were any and quantitatively to confirm cleaning of easily removable salts from the rock surface. Qualitative tests were performed by adding BaCl₂ to effluent samples to see any probable BaSO₄ precipitation. Quantitative tests performed by Ion Chromatography. Both quantitative and qualitative SO₄⁻² test results are presented in Appendix A.

5.2.2 Porosity Measurement

Cores dried at 90 °C to a constant weight. Dried cores weighted to measure w_{dry} . Cores then were saturated in a vacuum cell with de-ionized water. Porosity, ϕ , in fraction was calculated by using w_{dry} and $w_{saturated}$, in g, ρ_{DI} , in g/cm³ and V_{bulk} in cm³ of the core as shown in Equation 5.2

$$\varphi = \frac{W_{saturated}}{\frac{\rho_{DI}}{V_{bulk}}} \quad 5.2$$

Where,

- φ , the porosity of the core, fraction
- $W_{saturated}$, the weight of the saturated core, g
- ρ_{DI} , density of de-ionized water at 20 °C, g/cm³
- V_{bulk} , the bulk volume of the core, cm³

5.2.3 Permeability Measurement

Permeability measurements were performed in a flooding setup at room temperature with 8 bar of backpressure to ensure control over pressure difference, ΔP , between inlet and outlet. Each core flooded with de-ionized water with flow rates of 0.1 ml/min, 0.3 ml/min, and 0.5 ml/min. Pressure differences were recorded for corresponding flowrates and permeability, k in mD was calculated according to Equation 5.3

$$k = \frac{Q \mu L}{\Delta P A} \quad 5.3$$

where:

- k , the rock permeability, D
- Q , the flowrate, ml/s
- μ , viscosity of flooding fluid, cP,
- L , the length of the core, cm
- A , the cross-sectional flow area, cm²
- ΔP , the pressure difference between inlet and outlet, atm

After the permeability measurement, the core dried at 90 °C to a constant weight.

5.2.4 Establishing Initial Water Saturation

Knowing the dry weight of the core, target weight of the core with water saturation, $S_w=10\%$ were calculated as in Equation 5.4. The cleaned and dried core was fully saturated in a vacuum cell with 10 times diluted Valhall brine (d10VB0S)(Springer et al. 2003). A fully saturated core was placed in a desiccator with silica gel at the bottom to absorb water from the core. Core weight measured frequently until it reached the target weight. Once the core reached the target weight, the initial water saturation of 10% with VB0S was ensured to be established. After establishing initial water saturation, the core was secured in a sealed container to rest for 3 days to let the introduced brine diffuse all over the core.

$$w_{target} = w_{dry} + (0.1xPVx\rho_{VB0S}) \quad 5.4$$

where:

w_{target} , the weight of the core with $S_w=10\%$, g

w_{dry} , the weight of the dry core, g

PV, pore volume, ml

ρ_{VB0S} , density of the VB0S Brine, 1.0224 g/cm³

5.2.5 Establishing Oil Saturation

Core with $S_w=10\%$ was placed in a Hassler core holder in a heating set-up. The air in the pore space of the core was vacuumed before oil injection to provide an air-free oil saturation. After the vacuum was completed, 1 PV of Oil A was injected from both sides of the core with an injection rate of 0.165 ml/min. 2 PV of Oil A then was injected in direction of from right to left. Later 2 PV of Oil A was injected in direction of from left to right. After oil injection and flooding, the saturated core was weighted to confirm aimed oil saturation, $S_o=90\%$.

5.2.6 Aging Phase

Core with initial water and oil saturations wrapped in PTFE film tape to protect their constituents. Cores then were left aging at 130 °C for 14 days with a support cell filled with Oil A and pressurized to 10 bar to avoid evaporation or volatilization of the fluids.

5.2.7 Spontaneous Imbibition Test

Aged core placed in a steel imbibition cell filled with imbibing fluid connected to a piston cell filled with imbibing fluid and pressurized at 10 bar to provide pressure support. 10 bar of pressure support was important to keep fluids in the imbibition cell and core in the liquid phase at 130 °C of imbibing temperature. Produced oil was collected and oil volume was recorded to calculate Original Oil in Place, %OOIP.

5.2.8 CaCO₃-H₂SO₄ Batch Test

The batch test was performed to determine what maximum Ca⁺² and SO₄⁻² concentrations are possible without any precipitation in the pore water- H₂SO₄ - CaCO₃ system. The test was performed at 110 °C, 120 °C, and 130 °C and by adding 1 g of powdered rock into differently concentrated, 6mM; 8mM; 10mM; 12mM, H₂SO₄ solutions. Later samples were placed in a rotator setup in a heating system and let chemically equilibrate. After rock-acid interaction stabilized, samples were centrifuged and liquid phase filtered through 0.2 μm Pall Acrodisc filter. Filtered samples were analyzed in ion chromatography to determine ion concentrations, higher focus was done on Ca⁺² and SO₄⁻² in the samples. After determination maximum, possible concentrations were used to prepare the CaSO₄- Smart Water Brine.

6 Results

6.1 Core Cleaning

The results confirms that the ion concentration in effluents from core 1 is rather low (Figure 6.1), reaching a minimum concentration of ions after about 3.5 PV injection of DI water. Concentration of Mg^{+2} and K^{+} is low, while concentration of Ca^{+2} and SO_4^{-2} steadily declines and reach a minimum after about 3 PV injected. SO_4^{-2} is retained more strongly than Ca^{+2} .

With a low Mg^{+2} concentration, the salts present in the core material most likely have an origin of Gypsum/Anhydrite and not seawater.

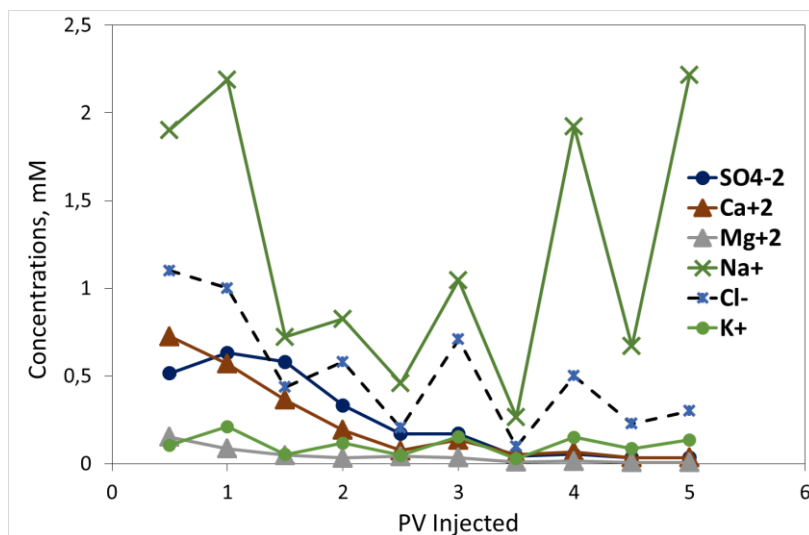


Figure 6.1 Core cleaning results for all ions for Core #1

The results from all the core cleaning experiments are summarized in Figure 6.2-Figure 6.7, confirming reproducible trends from core#1.

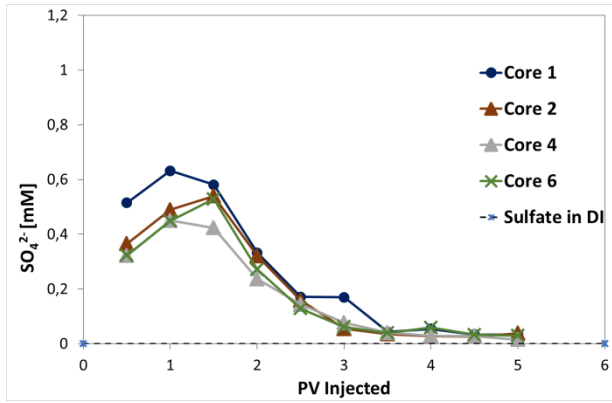


Figure 6.2 Ion chromatography results for core cleaning for $[SO_4^{2-}]$

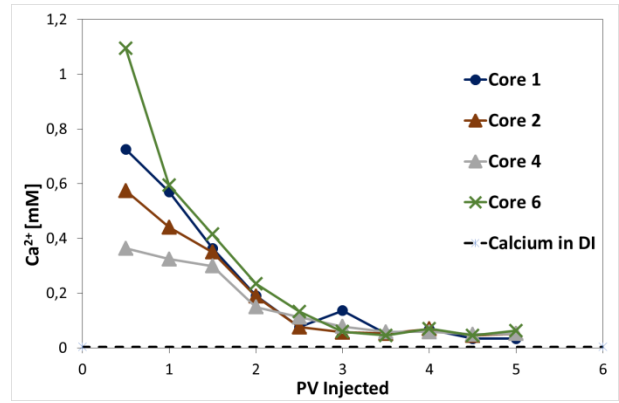


Figure 6.3 Ion chromatography results for core cleaning for $[Ca^{+2}]$

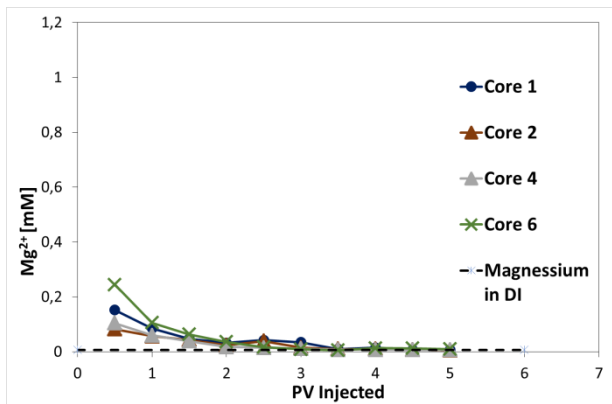


Figure 6.4 Ion chromatography results for core cleaning for $[Mg^{+2}]$

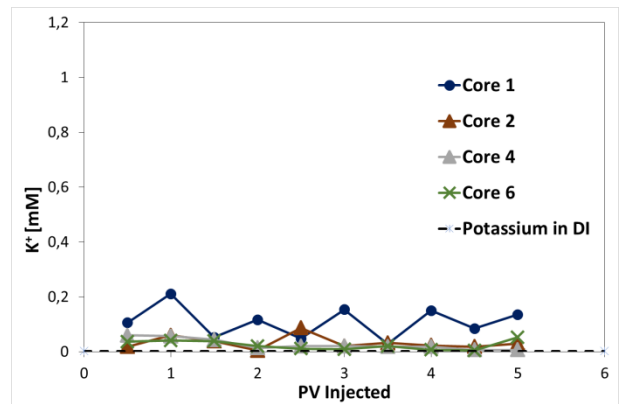


Figure 6.5 Ion chromatography results for core cleaning for $[K^{+}]$

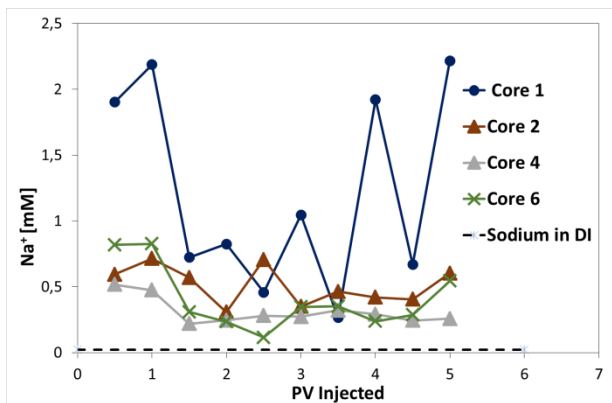


Figure 6.6 Ion chromatography results for core cleaning for $[Na^{+}]$

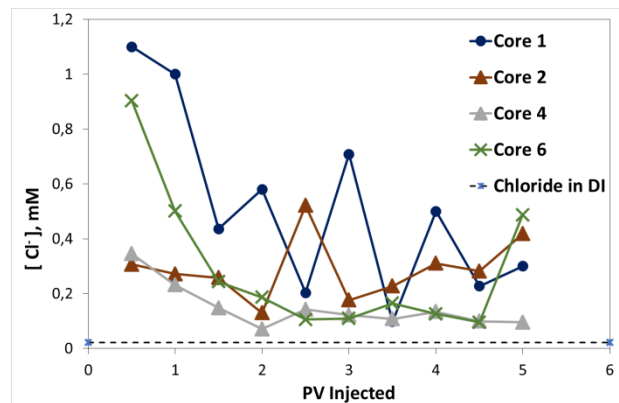


Figure 6.7 Ion chromatography results for core cleaning for $[Cl^{-}]$

6.2 Porosity and Permeability Measurement

6.2.1 Porosity Measurement

Rock porosities of the cores are measured according to Equation 6.1 and results are presented in presented in Table

$$\varphi = \frac{w_{saturated}}{V_{bulk} \rho_{DI}} \quad 6.1$$

Where,

- φ , the porosity of the core, fraction
- $w_{saturated}$, the weight of the saturated core, g
- ρ_{DI} , density of de-ionized water at 20 °C, g/cm³
- V_{bulk} , the bulk volume of the core, cm³

Table 6.1 Porosity Measurement Results

Core Name	Porosity (fraction)
Core #1	0.4778
Core #2	0.4807
Core #4	0.4741
Core #5	0.4410
Core #6	0.4707

6.2.2 Permeability Measurement

Rock permeabilities in this study were measured with a flooding setup. Cores were flooded with formation water with flow rates of 0.1 ml/min, 0.3 ml/min, and 0.5 ml/min. Corresponding pressure differences were recorded to calculate permeabilities according to Equation 5.3. Recorded pressure differences for corresponding flowrates and permeabilities are presented in Table 6.2.

$$k = \frac{Q \mu L}{\Delta P A} \quad 5.3$$

Where:

k , the rock permeability, D

Q , the flowrate, ml/s

μ , viscosity of flooding fluid, cP

L , the length of the core, cm

A , the cross-sectional flow area, cm²

ΔP , the pressure difference between inlet and outlet, atm

Table 6.2 Permeability Measurement Results

	Q,ml/min	ΔP , mbars	k, mD	Average k, mD
Core 1	0.1	235	4.14	4.08
	0.3	722	4.05	
	0.5	1200	4.06	
Core 2	0.1	239	3.99	4.00
	0.3	719	3.98	
	0.5	1182	4.04	
Core 4	0.1	267	3.63	3.61
	0.3	813	3.59	
	0.5	1349	3.60	
Core 5	0.1	258	3.77	3.77
	0.3	773	3.78	
	0.5	1290	3.77	
Core 6	0.1	251	3.94	3.93
	0.3	757	3.92	
	0.5	1263	3.92	

Table 6.3 summarizes porosities and permeabilities of the cores. The porosity values of the cores range between 0.4410 and 0.4807 while permeabilities of the cores range between 3.61-4.08 mD. Results presents that all the cores have similary porosity and permeabilities that can be considered high porosity and low permeability.

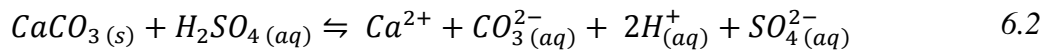
Table 6.3 Porosity and Permeability Summarized Results

Core Name	Porosity (fraction)	k (mD)
Core #1	0.4778	4.08
Core #2	0.4807	4.00
Core #4	0.4741	3.61
Core #5	0.4410	3.77
Core #6	0.4707	3.93

6.3 CaCO₃-H₂SO₄ Batch Test

A batch test was performed to determine the maximum possible SO₄⁻² and Ca⁺² concentration without causing precipitation. Maximum possible concentrations were used to prepare the CaSO₄-Smart Water brine. The batch test was performed at three different temperatures, 110 °C, 120 °C, and 130 °C.

Acidification reaction Equation 6.2 states that as H₂SO₄ concentration increases, equilibrium moves towards the right, and yields more products. After a critical value of sulfuric acid concentration, Equation 6.3 takes place in the right direction and CaSO₄ starts to precipitate.



Due to the endothermic nature of the reaction Equation 6.3, as temperature increases, equilibrium moves towards the right and yields more products meaning Equation 6.3 produces more reaction product in other words, causes CaSO₄ precipitation.

Results of the batch test are summarized in Table 6.4. The bold figures indicates the conditions that CaSO₄ precipitation happen.

Table 6.4 Ion Chromatography Analysis of the equilibrated $\text{CaCO}_3\text{-H}_2\text{SO}_4$ solutions

$\text{H}_2\text{SO}_4^{-2}$ [mM]	T=110 °C		T=120 °C		T=130 °C	
	SO_4^{-2} [mM]	Ca^{2+} [mM]	SO_4^{-2} [mM]	Ca^{2+} [mM]	SO_4^{-2} [mM]	Ca^{2+} [mM]
5.72	5.29	4.68	5.13	3.31	4.54	3.36
7.70	7.27	6.32	6.84	4.84	8.67	9.21
9.23	8.85	6.86	8.59	7.08	10.25	12.92
13.5	12.08	9.94	7.17	5.83	6.98	7.68

Figure 6.8 Free SO_4^{-2} concentration in $\text{CaCO}_3\text{-H}_2\text{SO}_4$ solutions.

shows how non-associated SO_4^{-2} concentration in the effluent samples changes as SO_4^{-2} concentration in bulk acid increases. As the figure illustrates, SO_4^{-2} concentration in the effluent samples increases as SO_4^{-2} concentration in bulk acid increases expectedly until a critical value of SO_4^{-2} concentration in bulk acid. After this critical value, even though SO_4^{-2} concentration in bulk acid continues to increase, SO_4^{-2} concentration in the effluent samples begin to decrease. This decrease indicates precipitation of SO_4^{-2} salts after the critical bulk acid concentration regarding dissolution reaction Equation 6.2.

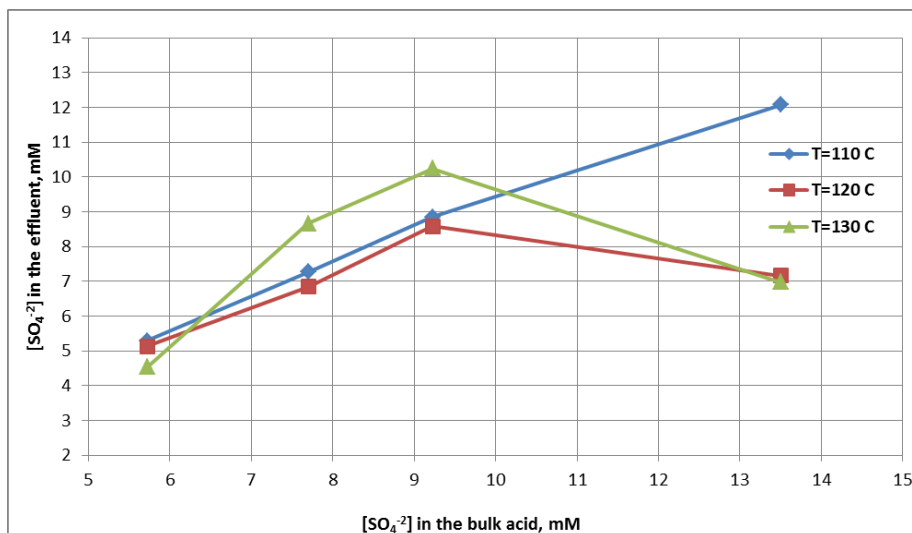


Figure 6.8 Free SO_4^{-2} concentration in $\text{CaCO}_3\text{-H}_2\text{SO}_4$ solutions.

Similarly, Figure 6.9 illuminates how Ca^{2+} concentration in the effluent samples changes as SO_4^{-2} concentration in bulk acid increases. The figure clarifies how Ca^{2+} concentration in the

effluent samples builds up as SO_4^{-2} concentration in bulk acid increases till it reaches a critical value of SO_4^{-2} concentration in bulk acid. After the critical value, Ca^{+2} concentration in the effluent samples starts to decrease rapidly. This rapid decrease shows precipitation of Ca^{+2} salts after the critical bulk acid concentration.

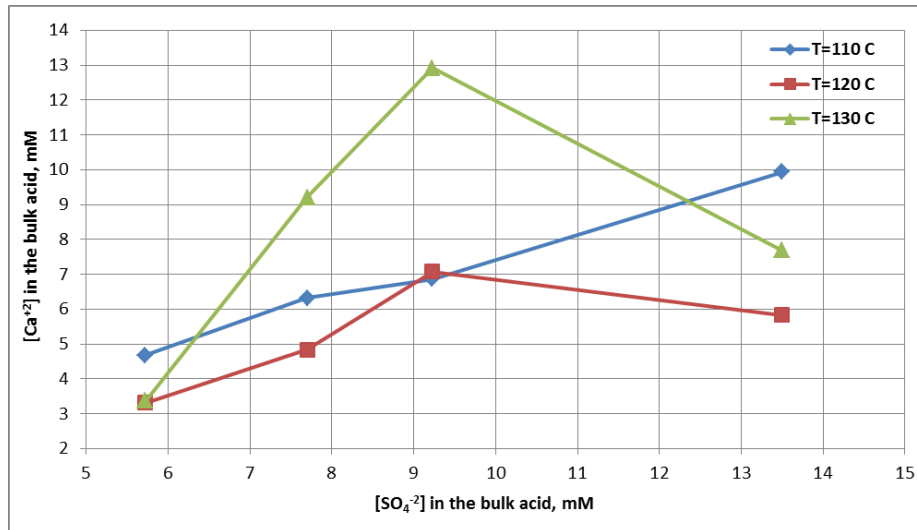


Figure 6.9 Free Ca^{+2} concentration in $\text{CaCO}_3\text{-H}_2\text{SO}_4$ solutions.

The precipitation of both SO_4^{-2} and Ca^{+2} salts can affect the porous system negatively not only due to damaging porous flow by decreasing porosity and permeability but also due to decreasing concentrations of potential determining ions like SO_4^{-2} and Ca^{+2} which are critical for wettability alteration by Smart Water processes in carbonates. Hence, determining maximum SO_4^{-2} and Ca^{+2} concentration that will not cause precipitation is important for Smartt Water desing.

The batch test results confirms that a maximum of 10 mM SO_4^{-2} could be present in solution before significant presipitation is observed. A sulfuric Acid based Smart Water for Chalk at 130 °C is the designed based on injection of 10 mM sulfuric acid solution.

6.4 The efficiency of a Sulfuric Acid Based Smart Water

The efficiency of a sulfuric acid-based smart water designed for 130 °C has been evaluated by spontaneous imbibition experiments at 130 °C.

Totally 4 cores have been restored with initial S_{wi} of 10%, and exposed to the same amount of crude oil with AN = 0.53 mgKOH/g and BN:0.31 mgKOH/g, to achieve the same initial core wettability.

The cores have then been spontaneously imbibed with different brines. FW was used to evaluate the initial core wettability after core restoration.

SW was used as an imbibing brine to evaluate the efficiency of SW for wettability alteration.

H_2SO_4 based $CaSO_4$ solution was used to evaluate if that could be used as a Smart Water at Ekofisk temperature of 130 C.

6.5 Spontaneous Imbibition

6.5.1 Initial core wettability

Spontaneous imbibition of the restored cores Core#1 and Core#6 was performed using FW as imbibing brine. The imbibing brine have the same composition as initially present brine in the restored cores to avoid any chemically induced wettability alteration processes during the experiments.

The results from the SI of core#1 is shown in Figure 6.10 The SI confirms an ultimate recovery of 31 % OOIP reached after 11 days

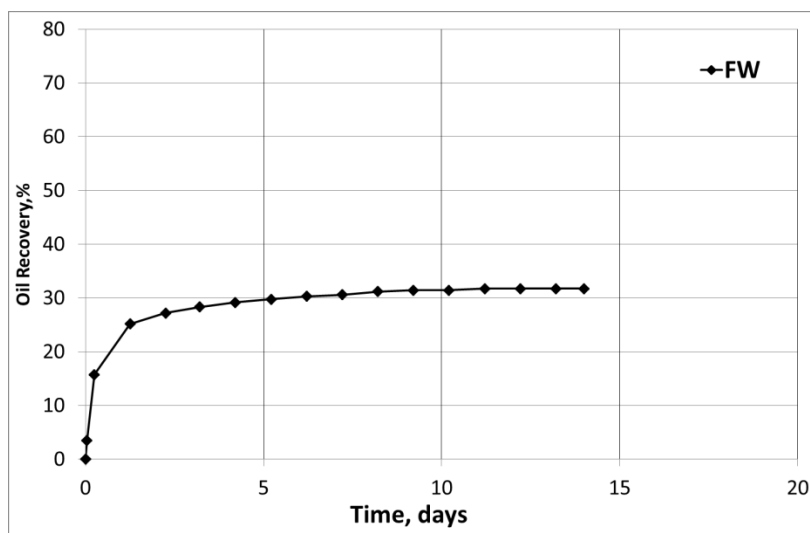


Figure 6.10 Oil Recovery with Spontaneous Imbibition by FW -Core#1

The spontaneous imbibition of core #6 with FW is presented in Figure 6.11.

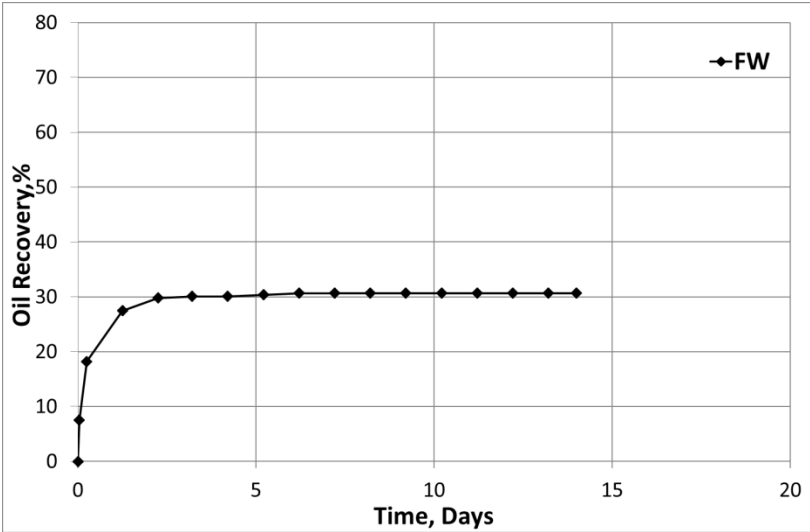


Figure 6.11 Oil Recovery with Spontaneous Imbibition by FW -Core#6

The results from Core #6 confirms the same ultimate recovery of 30 %OOIP, that Core#6 reached after 6 days

The SI experiments with formation Water (FW) confirms very good reproducibility in between the individual core experiments, and the same and slightly water wet core wettability can be expected in all the restored used cores in this work.

6.5.2 Tertiary Smart Water EOR Effects

After SI with FW in core #6, the imbining brine was changed to SW. Oil recovery result is presented in

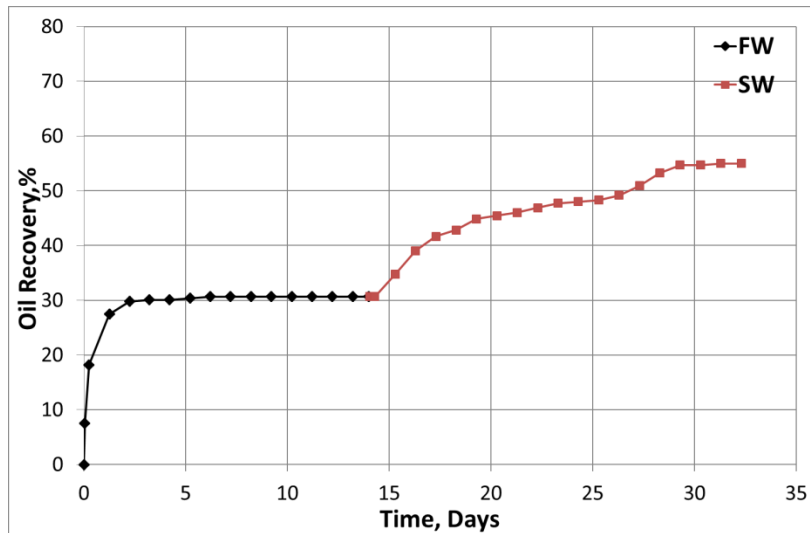


Figure 6.12 Oil Recovery with Spontaneous Imbibition by FW/SW -Core#6

The SI results presented in Figure 6.12 confirms that SW is able to change the initial core wettability, and a new ultimate recovery of 55% OOIP is produced in 13 days.

SW is used as the injection brine in Ekofisk field and should be regarded as the base line for water injection at Ekofisk for further injection brine modification.

The efficiency of CaSO_4 brine as a Smart Water in tertiary mode have been tested by changing the FW as the imbining brine of core #1 to 10 mM designed CaSO_4 brine.

The tertiary SI results on Core#1 is shown in Figure 3.1.

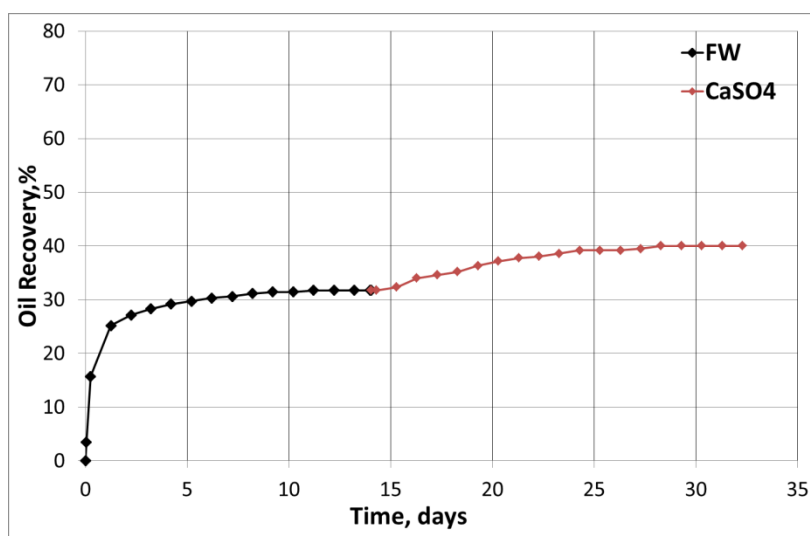


Figure 6.13 Oil recovery with spontaneous imbibition by FW/ CaSO_4 -Core#1

A slightly increase in oil recovery is observed using CaSO_4 brine, reaching an ultimate recovery of 40% after 15 days. The results present that, although CaSO_4 brine has a weak wettability alteration capability, CaSO_4 brine is significantly less efficient than SW.

6.5.3 Secondary Smart Water EOR Effects

The restored Core#2 was SI with SW in secondary mode. Oil Recovery results are presented in

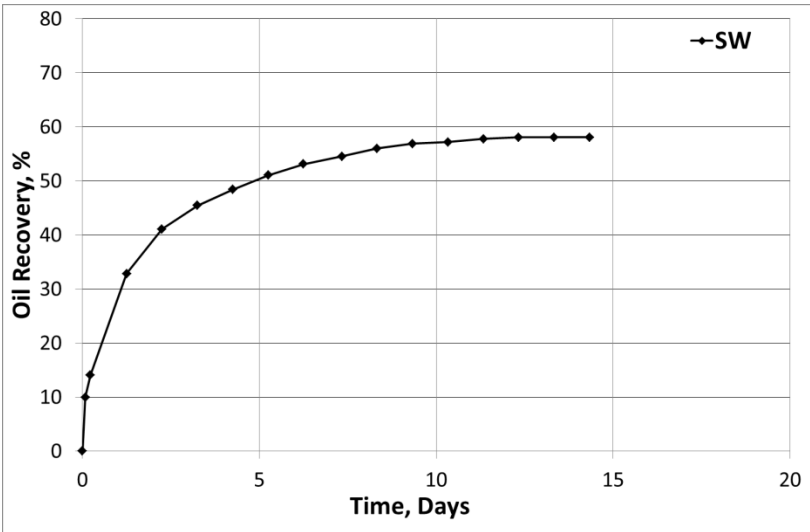


Figure 6.14 Oil recovery with spontaneous imbibition by SW- Core#2

Spontaneous imbibition for Core#2 resulted in an ultimate oil recovery of 58% of OOIP after 13 days, confirming that SW is extremely efficient as a Smart Water in chalk at high temperatures.

A tertiary experiments using the CaSO_4 brine after SW was planned but the experiment failed.

The restored core #4 was spontaneously imbibed with CaSO_4 brine in secondary mode. The results are presented in Figure 6.16

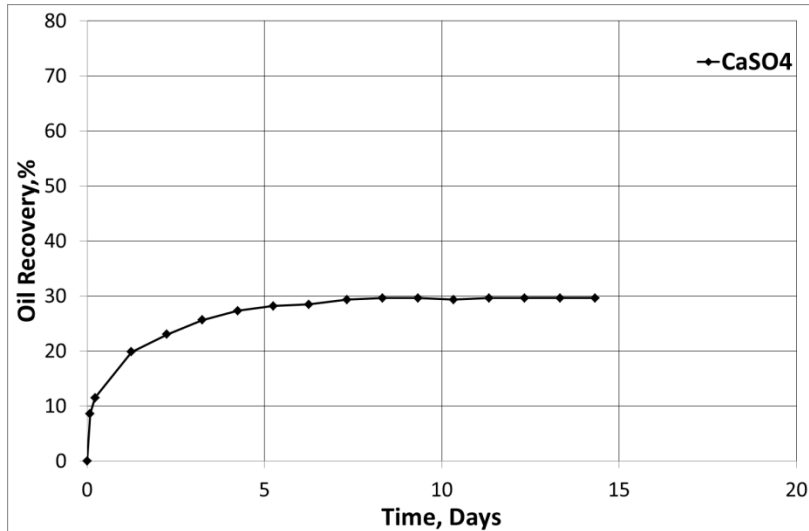


Figure 6.15 Oil recovery with spontaneous imbibition by CaSO₄

The ultimate recovery in this experiment gave a result of 30% OOIP after 8 days, close to the results achieved with FW in Core#1 and Core#6, confirming that CaSO₄ brine did not behave as a Smart Water in secondary mode at 130°C.

SW was then introduced as a Smart water in tertiary mode. A rapid and significant increase in recovery was observed, reaching an ultimate recovery of 54% OOIP after 8 days, validating that SW acts as a Smart Water in chalk at high temperatures Figure 6.16.

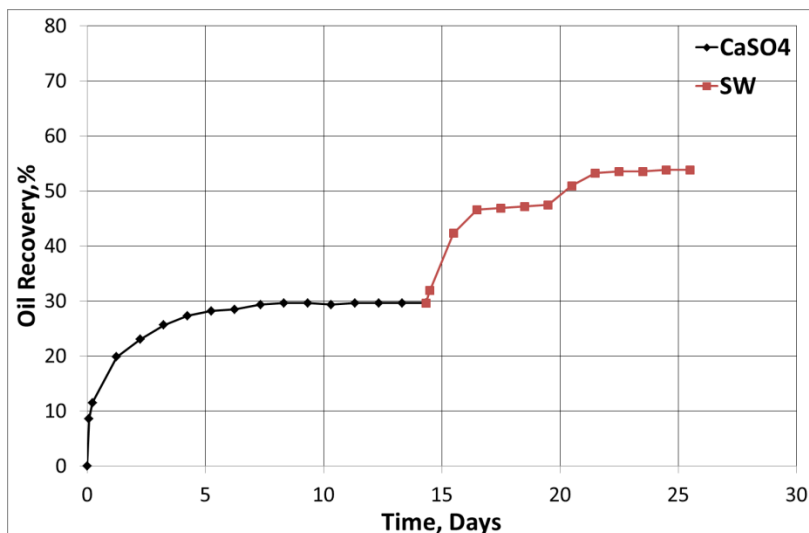


Figure 6.16 Oil recovery with spontaneous imbibition by CaSO₄/SW

6.5.4 Wettability Measurement

To quantify the water wetness of the cores used, spontaneous imbibition test results on the same SK Chalk were used (Andreassen et al., 2019). The test was performed on a precleaned SK Chalk core with 10% Swi. The core saturated with heptane then spontaneously imbibed by FW at 23 °C. The test results are presented in Figure 6.17, showing an ultimate recovery of 75% of OOIP.

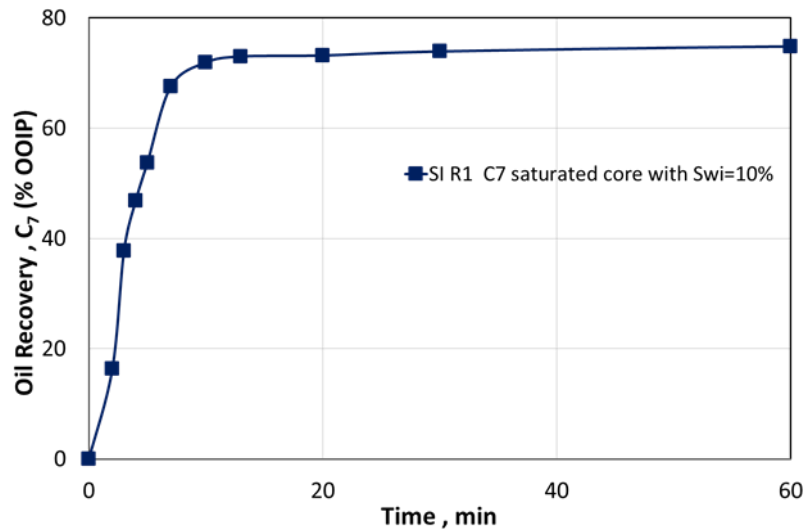


Figure 6.17 SI test results performed in a strongly water wet SK Chalk core

The core has a strongly water wet behaviour giving an ultimate recovery of 75% of OOIP that was reported to reach in the first 30 minutes. The results confirm strong capillary forces available.

Modified Amott index for Core #1 SI by FW as in Equation 6.4

$$I_{W-SI-Core\#1}^* = \frac{31.7}{75} = 0.42 \tag{6.4}$$

Modified Amott Indices are similarly calculated as above and presented in Table 6.5.

Table 6.5 Oil Recovery by Spontaneous Imbibition on Secondary and Tertiary Mode at 130 °C

	Secondary Mode		Tertiary Mode	
	Imbibing Fluid	I_{W-SI}^*	Imbibing Fluid	I_{W-SI}^*
Core 1	FW	0.42	CaSO ₄	0.54
Core 6	FW	0.41	SW	0.73
Core 2	SW	0.78	CaSO ₄	<i>Failed</i>
Core 4	CaSO ₄	0.39	SW	0.72

Table 6.5 shows the water wettesses of the cores. Initial water wetness of the cores are and reproduced around 0.4. The results confirms that seawater modifies wettability towards more water wet states in both secondary and tertiary mode. In addition, although CaSO₄ brine is able change wettability towards water wet, it does not show a strong modifier effect.

7 Discussions

All SK outcrop cores was precleaned in front of the experimets to avoid ion polutions in the outcrop material affecting core restoration.

The results confirms that quite similar porosity and permeability properties exist in all cores used.

Core restorations was performed with S_{wi} of 10% and by exposing the cores to equal amouts of crude oil, Oil A, with AN of 0.53 mgKOH/g.and BN of 0.31 mgKOH/g The SI experimets with FW confirmed reproducible wettabilty results.

SW behaves as a Smart Water at high temperatures in Chalk. Ca^{+2} and SO_4^{-2} ions are the main ions contributing in the wettability alteration process.

A Smart Water EOR brine that could easily be designed by using low concentrations of sulfuric acid in fresh water. Such a brine was tested and compared to SW as an injection brine.It is confirmed by the batch test that the $CaSO_4$ brine can have a maximum of 10 mM concentration of SO_4^{-2} in solution at 130 °C,

The results in this work also validates that SW is a Smart Water in Chalk at 130°C and very efficently change the core wettability towards more water wet conditions.

The designed $CaSO_4$ brine did not behave as a Smart Water, neither in secondary nor in tertiary mode after FW. The reason for this is not cleary shown with these results. The SO_4^{-2} concentration is significantly lower compared to SW and could be the explanation for this.

Knowing SW has more SO_4^{-2} than $CaSO_4$ brine and performing well without causing significant precipitation, to be able increase SO_4^{-2} concentration of $CaSO_4$ brine with no precipitation, other ions present in SW should be researched and considered to be added to $CaSO_4$ brine.

If increasing SO_4^{-2} concentration in a $CaSO_4$ brine is targeted, it is likely that Mg^{+2} ions need to be added to the brine composition. Mg^{+2} ions are most likely to stabilize the ionic environment in the brine and avoid $CaSO_4$ precipitation by complexing SO_4^{-2} with Mg^{+2} , $Mg^{+2}:SO_4^{-2}$

Mg^{+2} concentration in SW is 45 mM, but could probably be significantly reduced, i.e. 24 mM which is equal to the SO_4^{-2} concentration in SW. The optimal Mg^{+2} concentration in a brine involving Mg^{+2} , Ca^{+2} , and SO_4^{-2} needs to be experimentally investigated in further studies.

8 Conclusion

The main conclusions observed from this study are as follows.

Table 8.1 Oil Recovery by Spontaneous Imbibition on Secondary and Tertiary Mode at 130 °C

	Secondary Mode		Tertiary Mode	
	Imbibing Fluid	%OOIP	Imbibing Fluid	%OOIP
Core 1	FW	31.7	CaSO ₄	40.1
Core 6	FW	30.7	SW	55.0
Core 2	SW	58.1	CaSO ₄	<i>Terminated</i>
Core 4	CaSO ₄	29.6	SW	53.8

- The study suggested 10 mM CaSO₄ solution as a Smart Water that can alter wettability in chalk carbonate at 130 °C. The Smart Water concentration was decided after the CaCO₃-H₂SO₄ batch test to contain maximum Ca⁺² and SO₄⁻² without causing any precipitation.
- The Smart Water was tested as the spontaneous imbibition fluid to see any possible wettability altering effects. For Core#1, Smart Water was used in tertiary mode after FW and resulted in extra oil recovery of 8.4% of OOIP. This extra oil recovery indicates that the wettability altering capability of the Smart Water is not powerful but exists.
- Seawater also was tested as the spontaneous imbibition fluid to observe any possible wettability modifying effects. For Core#6, seawater was used in tertiary mode after FW, and extra oil recovery of 24.3% of OOIP was reported. This extra oil recovery confirmed that seawater can alter wettability in favor of oil displacement.
- Smart Water was used as a spontaneous imbibition fluid in the secondary mode as well. The experiment resulted in 29.6% of OOIP oil recovery.
- Seawater also was used as a spontaneous imbibition fluid in the secondary mode and the experiment resulted in 58.1% of OOIP oil recovery
- Seawater was used as an imbibing fluid in tertiary mode after Smart Water to see if seawater can alter wettability in a Smart Water imbibed core. Core#4 was spontaneously imbibed with Smart Water and resulted in 29.6% OOIP oil

recovery. Then imbibing fluid was changed to seawater and 53.8% of OOIP oil was recovered. This extra 24.2% of OOIP oil recovery indicates that seawater is a wettability modifier even after Smart Water.

Appendixes

Spontaneous Imbibition Data

Core#1

Time, Days	Oil Volume, mL	Oil Recovery, %
0	0	0
0,04	1,2	3,431120261
0,25	5,5	15,72596786
1,25	8,8	25,16154858
2,25	9,5	27,1630354
3,21	9,9	28,30674215
4,21	10,2	29,16452222
5,21	10,4	29,73637559
6,21	10,6	30,30822897
7,21	10,7	30,59415566
8,21	10,9	31,16600904
9,21	11	31,45193572
10,21	11	31,45193572
11,21	11,1	31,73786241
12,21	11,1	31,73786241
13,21	11,10	31,73786241
14,00	11,10	31,73786241
14,04	11,1	31,73786241
14,29	11,1	31,73786241
15,29	11,3	32,30971579
16,29	11,9	34,02527592
17,29	12,1	34,5971293
18,29	12,3	35,16898267
19,29	12,7	36,31268943
20,29	13	37,17046949
21,29	13,2	37,74232287
22,29	13,3	38,02824956

23,29	13,5	38,60010293
24,29	13,7	39,17195631
25,29	13,7	39,17195631
26,29	13,7	39,17195631
27,29	13,8	39,457883
28,29	14	40,02973638
29,29	14	40,02973638
30,29	14	40,02973638
31,29	14	40,02973638
32,29	14	40,02973638
Time, Days	Oil Volume, mL	Oil Recovery, %

Core #2

Time, Days	oil volume, mL	oil recovery, %
0	0	0
0,083333333	3,4	9,975647684
0,229166667	4,8	14,08326732
1,25	11,2	32,86095708
2,25	14	41,07619634
3,25	15,5	45,47721738
4,25	16,5	48,41123141
5,25	17,4	51,05184403
6,25	18,1	53,10565385
7,333333333	18,6	54,57266086
8,333333333	19,1	56,03966787
9,333333333	19,4	56,91987208
10,33333333	19,5	57,21327348
11,33333333	19,7	57,80007628
12,33333333	19,8	58,09347769
13,33333333	19,8	58,09347769
14,33333333	19,8	58,09347769
Time, Days	oil volume, mL	oil recovery, %

Core #4

Time, Days	oil volume, mL	oil recovery, %
0	0	0
0,0833333	3	8,633341967
0,2291667	4	11,51112262
1,25	6,9	19,85668652
2,25	8	23,02224524
3,25	8,9	25,61224783
4,25	9,5	27,33891623
5,25	9,8	28,20225042
6,25	9,9	28,49002849
7,3333333	10,2	29,35336269
8,3333333	10,3	29,64114075
9,3333333	10,3	29,64114075
10,333333	10,2	29,35336269
11,333333	10,3	29,64114075
12,333333	10,3	29,64114075
13,333333	10,3	29,64114075
14,333333	10,3	29,64114075
14,5	11,1	31,94336528
15,5	14,7	42,30337564
16,5	16,2	46,62004662
17,5	16,3	46,90782469
18,5	16,4	47,19560275
19,5	16,5	47,48338082
20,5	17,7	50,9367176
21,5	18,5	53,23894213
22,5	18,6	53,52672019
23,5	18,6	53,52672019
24,5	18,7	53,81449826
25,5	18,7	53,81449826
Time, Days	oil volume, mL	oil recovery, %

Core#6

Time, Days	oil volume, mL	oil recovery, %
0	0	0
0,0416667	2,6	7,523148148
0,25	6,3	18,22916667
1,25	9,5	27,48842593
2,25	10,3	29,80324074
3,2083333	10,4	30,09259259
4,2083333	10,4	30,09259259
5,2083333	10,5	30,38194444
6,2083333	10,6	30,6712963
7,2083333	10,6	30,6712963
8,2083333	10,6	30,6712963
9,2083333	10,6	30,6712963
10,208333	10,6	30,6712963
11,208333	10,6	30,6712963
12,208333	10,6	30,6712963
13,208333	10,6	30,6712963
14	10,6	30,6712963
14,041667	10,6	30,6712963
14,291667	10,6	30,6712963
15,291667	12	34,72222222
16,291667	13,5	39,0625
17,291667	14,4	41,66666667
18,291667	14,8	42,82407407
19,291667	15,5	44,84953704
20,291667	15,7	45,42824074
21,291667	15,9	46,00694444
22,291667	16,2	46,875
23,291667	16,5	47,74305556
24,291667	16,6	48,03240741
25,291667	16,7	48,32175926
26,291667	17	49,18981481

27,291667	17,6	50,92592593
28,291667	18,4	53,24074074
29,291667	18,9	54,6875
30,291667	18,9	54,6875
31,291667	19	54,97685185
32,291667	19	54,97685185
Time, Days	oil volume, mL	oil recovery, %

8.1 Core Cleaning Data

Core#1

PV of DI Flooded	[SO ₄ ⁻²]	[Ca ⁺²]	[Mg ⁺²]	[K ⁺]	[Na ⁺]	[Cl ⁺²]
0.5	0,514885	0,725449	0,152282	0,10536	1,902213304	1,663671
1.0	0,631663	0,569839	0,085589	0,210719	2,188084679	1,793518
1.5	0,580705	0,36382	0,047797	0,05268	0,722769138	0,436206
2.0	0,332286	0,190677	0,032235	0,116812	0,825251329	0,580256
2.5	0,170921	0,075613	0,042239	0,048099	0,458472961	0,202887
3.0	0,169859	0,135885	0,034458	0,153459	1,04639711	0,809518
3.5	0,043526	0,051505	0,010004	0,027485	0,266094111	0,097386
4.0	0,054143	0,067942	0,01445	0,15	1,921990569	1,756999
4.5	0,033972	0,033971	0,006669	0,084746	0,668831143	0,227233
5.0	0,023272	0,023171	0,004549	0,135135	2,21685161	4,455392

Core#2

PV of DI Flooded	[SO ₄ ⁻²]	[Ca ⁺²]	[Mg ⁺²]	[K ⁺]	[Na ⁺]	[Cl ⁺²]
0.5	0,365197	0,574222	0,082255	0,018323	0,595115882	0,306359
1.0	0,489406	0,440529	0,056689	0,059551	0,713779472	0,271868
1.5	0,539302	0,349574	0,04335	0,038937	0,569944818	0,257666
2.0	0,320609	0,188485	0,023343	0,004581	0,307446574	0,129847
2.5	0,158181	0,075613	0,038904	0,087036	0,70658774	0,521419
3.0	0,055204	0,056984	0,01445	0,020614	0,35059697	0,176511
3.5	0,035033	0,052601	0,010004	0,032066	0,46386676	0,227233
4.0	0,027602	0,069038	0,010004	0,022904	0,420716364	0,310417
4.5	0,02654	0,04493	0,007781	0,018323	0,404534965	0,282013
5.0	0,038218	0,051505	0,005558	0,029776	0,604105548	0,417947

Core#4

PV of DI Flooded	[SO ₄ ⁻²]	[Ca ⁺²]	[Mg ⁺²]	[K ⁺]	[Na ⁺]	[Cl ⁺²]
0.5	0,32167	0,36382	0,104486	0,059551	0,517804756	0,344907
1.0	0,450126	0,32437	0,060024	0,057261	0,474654359	0,231291
1.5	0,423586	0,299165	0,038904	0,043518	0,219347848	0,148107
2.0	0,236741	0,149035	0,017785	0,013743	0,246316846	0,07101
2.5	0,143318	0,111776	0,01445	0,020614	0,280477576	0,142021
3.0	0,076437	0,077805	0,011116	0,020614	0,273285843	0,121732
3.5	0,040341	0,05808	0,007781	0,018323	0,321830039	0,10753
4.0	0,028664	0,05808	0,007781	0,018323	0,291265175	0,133905
4.5	0,027602	0,049313	0,006669	0,006871	0,244518912	0,099414
5.0	0,014863	0,051505	0,006669	0,006871	0,257104445	0,095357

Core#6

PV of DI Flooded	[SO ₄ ⁻²]	[Ca ⁺²]	[Mg ⁺²]	[K ⁺]	[Na ⁺]	[Cl ⁺²]
0.5	0,322732	1,094748	0,244541	0,036647	0,818059597	0,902846
1.0	0,449064	0,593948	0,105597	0,041228	0,827049263	0,50113
1.5	0,528686	0,415325	0,063358	0,038937	0,309244507	0,243464
2.0	0,271774	0,234511	0,03557	0,020614	0,235529247	0,186656
2.5	0,128456	0,132597	0,016673	0,011452	0,115067723	0,105501
3.0	0,061574	0,059176	0,008892	0,009162	0,347001104	0,109559
3.5	0,03928	0,04493	0,005558	0,020614	0,352394903	0,164338
4.0	0,059451	0,070134	0,013339	0,006871	0,23732718	0,12579
4.5	0,03291	0,04493	0,012227	0,004581	0,285871376	0,095357
5.0	0,029725	0,062463	0,010004	0,05268	0,544773753	0,486928

Bibliography

- Al-Maamari, R. S. H., & Buckley, J. S. (2013). Asphaltene Precipitation and Alteration of Wetting: The Potential for Wettability Changes During Oil Production. *SPE reservoir evaluation & engineering*, 6(4), 210-214. <https://doi.org/10.2118/84938-pa>
- Alvarez, J. M., & Sawatzky, R. P. (2013, 2013/6/11/). *Waterflooding: Same Old, Same Old?* SPE Heavy Oil Conference-Canada, Calgary, Alberta, Canada. <https://doi.org/10.2118/165406-MS>
- Amott, E. (1959). Observations Relating to the Wettability of Porous Rock. *Transactions of the AIME*, 216(01), 156-162. <https://doi.org/10.2118/1167-G>
- Anderson, W. G. (1986). Wettability Literature Survey- Part 1: Rock/Oil/Brine Interactions and the Effects of Core Handling on Wettability. *Journal of petroleum technology*, 38(10), 1125-1144. <https://doi.org/10.2118/13932-PA>
- Anderson, W. G. (2013). Wettability Literature Survey- Part 1: Rock/Oil/Brine Interactions and the Effects of Core Handling on Wettability. *Journal of petroleum technology*, 38(10), 1125-1144. <https://doi.org/10.2118/13932-pa>
- [Record #90 is using a reference type undefined in this output style.]
- Buckley, J. S. (1996). *Mechanisms and consequences of wettability alteration by crude oils* [Department of Petroleum Engineering, Heriot-Watt University]. Edinburgh.
- Buckley, J. S., & Liu, Y. (1998). Some mechanisms of crude oil/brine/solid interactions. *Journal of Petroleum Science and Engineering*, 20(3), 155-160. [https://doi.org/https://doi.org/10.1016/S0920-4105\(98\)00015-1](https://doi.org/https://doi.org/10.1016/S0920-4105(98)00015-1)
- Buckley, J. S., Takamura, K., & Morrow, N. R. (2013). Influence of Electrical Surface Charges on the Wetting Properties of Crude Oils. *SPE reservoir engineering*, 4(3), 332-340. <https://doi.org/10.2118/16964-pa>
- Chilingar, G. V., & Yen, T. F. (1983). Some Notes on Wettability and Relative Permeabilities of Carbonate Reservoir Rocks, II. *Energy Sources*, 7(1), 67-75. <https://doi.org/10.1080/00908318308908076>
- Cook, T. A. (2013). *Reserve growth of oil and gas fields—Investigations and applications* [Report](2013-5063). (Scientific Investigations Report, Issue. U. S. G. Survey. <http://pubs.er.usgs.gov/publication/sir20135063>
- Craig, F. F. (1971). *The reservoir engineering aspects of waterflooding* (Vol. vol. 3). Henry L. Doherty Memorial Fund of AIME.
- Cuiec, L. (1984, 1984/1/1/). *Rock/Crude-Oil Interactions and Wettability: An Attempt To Understand Their Interrelation* SPE Annual Technical Conference and Exhibition, Houston, Texas. <https://doi.org/10.2118/13211-MS>

- Denekas, M. O., Mattax, C. C., & Davis, G. T. (1959). Effects of Crude Oil Components on Rock Wettability. *Transactions of the AIME*, 216(01), 330-333. <https://doi.org/10.2118/1276-G>
- Green, D. W., & Willhite, G. P. (1998). *Enhanced oil recovery* (Vol. vol. 6). Henry L. Doherty Memorial Fund of AIME, Society of Petroleum Engineers.
- Hirasaki, G. J. (1991). Wettability: Fundamentals and Surface Forces. *SPE formation evaluation*, 6(2), 217-226. <https://doi.org/10.2118/17367-PA>
- Jadhunandan, P. P., & Morrow, N. R. (2013). Effect of Wettability on Waterflood Recovery for Crude-Oil/Brine/Rock Systems. *SPE reservoir engineering*, 10(1), 40-46. <https://doi.org/10.2118/22597-pa>
- [Record #6 is using a reference type undefined in this output style.]
- Kowalewski, E., Boassen, T., & Torsæter, O. (2003). Wettability alterations due to aging in crude oil; wettability and Cryo-ESEM analyses. *Journal of Petroleum Science and Engineering - J PET SCI ENGINEERING*, 39, 377-388. [https://doi.org/10.1016/S0920-4105\(03\)00076-7](https://doi.org/10.1016/S0920-4105(03)00076-7)
- Letellier, P., Mayaffre, A., & Turmine, M. (2007). Drop size effect on contact angle explained by nonextensive thermodynamics. Young's equation revisited. *Journal of Colloid and Interface Science*, 314(2), 604-614. <https://doi.org/https://doi.org/10.1016/j.jcis.2007.05.085>
- [Record #27 is using a reference type undefined in this output style.]
- Menezes, J., Yan, J., & Sharma, M. (1989). The Mechanism of Wettability Alteration Due to Surfactants in Oil-Based Muds. <https://doi.org/10.2118/18460-MS>
- Moore, T. F., & Slobod, R. L. (1955, 1955/1/1). *Displacement of Oil by Water-Effect of Wettability, Rate, and Viscosity on Recovery* Fall Meeting of the Petroleum Branch of AIME, New Orleans, Louisiana. <https://doi.org/10.2118/502-G>
- Muggeridge, A., Cockin, A., Webb, K., Frampton, H., Collins, I., Moulds, T., & Salino, P. (2014). Recovery rates, enhanced oil recovery and technological limits. *Philos Trans A Math Phys Eng Sci*, 372(2006), 20120320-20120320. <https://doi.org/10.1098/rsta.2012.0320>
- Pierre, A., Lamarche, J. M., Mercier, R., Foissy, A., & Persello, J. (1990). CALCIUM AS POTENTIAL DETERMINING ION IN AQUEOUS CALCITE SUSPENSIONS. *Journal of Dispersion Science and Technology*, 11(6), 611-635. <https://doi.org/10.1080/01932699008943286>
- Punternvold, T. (2008). *Waterflooding of carbonate reservoirs : EOR by wettability alteration* University of Stavanger, Faculty of Science and Technology, Department of Petroleum Engineering]. Stavanger.
- Standnes, D. C. (2001). *Enhanced oil recovery from oil-wet carbonate rock by spontaneous imbibition of aqueous surfactant solutions* Norges teknisk-naturvitenskapelige universitet, Petroleumsteknologi og anvendt geofysikk]. Trondheim.
- Strand, S. (2005). *Wettability alteration in chalk : a study of surface chemistry* University of Stavanger]. Stavanger.

- Strand, S., Høgenesen, E. J., & Austad, T. (2006). *Colloids Surf., A*, 275, 1.
- Strand, S., Puntervold, T., & Austad, T. (2008). Effect of Temperature on Enhanced Oil Recovery from Mixed-Wet Chalk Cores by Spontaneous Imbibition and Forced Displacement Using Seawater. *Energy & Fuels*, 22(5), 3222-3225. <https://doi.org/10.1021/ef800244v>
- Strand, S., Standnes, D., & Austad, T. (2006). New wettability test for chalk based on chromatographic separation of SCN⁻ and SO₄²⁻. *Journal of Petroleum Science and Engineering - J PET SCI ENGINEERING*, 52, 187-197. <https://doi.org/10.1016/j.petrol.2006.03.021>
- [Record #7 is using a reference type undefined in this output style.]
- Torsæter, O., & Silseth, J. K. (1985). *The effects of sample shape and boundary conditions on capillary imbibition*.
- Treiber, L. E., & Owens, W. W. (1972). A Laboratory Evaluation of the Wettability of Fifty Oil-Producing Reservoirs. *Society of Petroleum Engineers journal*, 12(6), 531-540. <https://doi.org/10.2118/3526-PA>
- Wade, J. E. (1971, 1971/1/1). *Some Practical Aspects of Waterflooding* 8th World Petroleum Congress, Moscow, USSR. <https://doi.org/>
- Yuan, Y., & Lee, T. R. (2013). Contact Angle and Wetting Properties. In G. Bracco & B. Holst (Eds.), *Surface Science Techniques* (pp. 3-34). Springer Berlin Heidelberg. https://doi.org/10.1007/978-3-642-34243-1_1
- Zhang, P. (2006). *Water-based EOR in fractured chalk : wettability and chemical additives* University of Stavanger, Faculty of Science and Technology, Department of Petroleum Engineering]. Stavanger.
- Zhang, P., & Austad, T. (2006). *Colloids Surf., A*, 279, 179.
- Zhang, P., Tweheyo, M. T., & Austad, T. (2007a). *Colloids Surf., A*, 301, 199.
- Zhang, P., Tweheyo, M. T., & Austad, T. (2007b). Wettability alteration and improved oil recovery by spontaneous imbibition of seawater into chalk: Impact of the potential determining ions: Ca²⁺, Mg²⁺ and SO₄²⁻. *Colloids Surf., A*, 301, 199.
- Zhou, X., Morrow, N., Of, U., Ma, S., & Research, W. (1996). Interrelationship of Wettability, Initial Water Saturation, Aging Time, and Oil Recovery by Spontaneous Imbibition and Waterflooding. *SPE Journal*, 5. <https://doi.org/10.2118/35436-MS>